WATER RESOURCES RESEARCH, VOL. 49, 4379–4398, doi:10.1002/wrcr.20369, 2013

Evaluation of the effects of temperature changes on fine timescale rainfall

Yeboah Gyasi-Agyei[1]

Received 27 January 2013; revised 8 May 2013; accepted 16 June 2013; published 29 July 2013.

[1] An enhanced copula-based daily rainfall disaggregation model is presented. The rainfall data are grouped into maximum daily temperature quantiles instead of the usual monthly grouping in order to account for seasonal temperature shifts. Empirical and statistical evidence provided supports the conditioning of the model parameters on temperature. Linkage of the major model parameters to maximum daily temperature allows easy evaluation of temperature changes on fine timescale rainfall statistics. Rainfall data sets for three Australian capital cities located in different climatic regions were used to test the applicability of the presented model. It is observed that statistics such as the total wet periods' duration, storm event duration, and the autocorrelations decrease with increase in temperature, while the maximum wet period depth, variance, skewness, and the intensity-duration-frequency (IDF) show an increasing trend with temperature. Considering the 24 h wet day rainfall data sets, a 1°C rise in temperature could cause rates of change, depending on the climate (lowest rates for cool temperate zones and highest for the hot tropics), of 2%–14% in the total wet periods' duration, 5%–16% in variance, 10%–30% in skewness, 5%–9% in maximum period depth (including IDF), and 4%–25% in autocorrelations. Simulating single events of varying depths, and using temperature values spanning the spectrum of the recorded data for the capital cities, the average rates were 2%–12% for duration (and total wet periods' duration), 10%–26% for variance, 20%–32% for skewness and 1%–20% for the autocorrelations, all of which match the 24 h wet day results very well.

Citation: Gyasi-Agyei, Y. (2013), Evaluation of the effects of temperature changes on fine timescale rainfall, *Water Resour. Res.*, *49*, 4379–4398, doi:10.1002/wrcr.20369.

1. Introduction

[2] Rainfall is a complicated mechanism involving rising and cooling of air, moisture availability, cloud development and condensation, as well as the growth of cloud droplets. These processes are influenced by the atmospheric covariates of temperature, relative humidity, pressure, and wind speed over land masses and the oceans. It has been established that the ocean-atmospheric processes, El-Nino/Southern Oscillation (ENSO), Interdecadal Pacific Oscillation (IPO), Indian Ocean Dipole (IOD), and Southern Annular Mode (SAM) influence the hydroclimatology of Australia. An extensive review of these large-scale climate drivers in relation to Australia has been provided by *Gallant et al*. [2012] and *Ho et al*. [2012]. While they may influence the rainfall up to the daily timescale, no information is available on their direct effect on subdaily or subhourly rainfall statistics. Since our attention is focused on disaggregation of daily to subdaily timescale, atmospheric variables of temperature, relative humidity, pressure, and wind speed that are measured on a daily basis are of consideration. However, there is a very strong dependence of all of these variables with temperature [e.g., *Wooten*, 2011]. Hence, temperature is the only predictor of interest in this paper.

[3] Temperature is the driving force of the hydrologic cycle and therefore has a profound effect on rainfall characteristics. Increased temperature increases evaporation with the consequence of increased drought severity. By the same token, the Clausius-Clapeyron equation estimates that an increase of 1°C in temperature causes 7% increase in the water holding capacity of the air masses which results in more intense rainfall, increasing the risk of flooding, erosion, and water damage. The risk of high intensity rainfall associated with global warming has even been speculated for most subtropical and midlatitude regions where mean regional rainfall decreases with temperature [e.g., *Meehl et al*., 2007; *Trenberth*, 2011]. Available research on the linkage of temperature and rainfall has focused on the extreme rainfall (particularly 99th percentile and above) and a few at the subdaily timescale [e.g., *Hardwick-Jones et al*., 2010; *Berg et al*., 2009]. This paper is interested in the temperature scaling for all rainfall percentiles as continuous rainfall simulation demands.

[1]Centre for Railway Engineering, School of Engineering and Technology, Central Queensland University, Rockhampton, Queensland, Australia.

Corresponding author: Y. Gyasi-Agyei, Centre for Railway Engineering and School of Engineering and Technology, Central Queensland University, Rockhampton, QLD 4702, Australia. (y.gyasi-agyei@cqu.edu.au)

0043-1397/13/10.1002/wrcr.20369

[4] Availability of long records of high-resolution continuous timescale rainfall data is crucial for modeling and understanding runoff, erosion, and chemical transport within urban environments that experience flash flooding. This is also true for agricultural landscapes where changes in the environmental processes occur as a result of the high intensities of fine timescale rainfall. However, there is a worldwide shortage of long records of fine timescale continuous rainfall data, particularly in the third world. In recent years radar technology is being used to gather high-resolution rainfall data, but they are of short record length and there is also a high uncertainty in the algorithms used for converting the radiometric measurements into rainfall [e.g., *Krajewski et al*., 2010]. In contrast to limited fine timescale rainfall data availability, long records of daily rainfall data are freely available online in many countries. Typical examples are the dense network of over 100 years of daily rainfall data maintained by the Australian Bureau of Meteorology (http://www.bom.gov.au/climate/data/) and the Australian Silo Data Drill facility that generates long daily rainfall records (http://www.longpaddock.qld.gov.au/silo/).

[5] To overcome the scarcity of high-resolution rainfall data, research efforts have been focused on disaggregating the available long records of daily rainfall into fine timescale. In this way, the annual and seasonal trends that are difficult to generate stochastically are preserved. Notable examples of research efforts in this direction include *Hershenhorn and Woolhiser* [1987], *Econopouly et al*. [1990], *Bo et al*. [1994], *Glasbey et al*. [1995], *Cowpertwait et al*. [1996], *Gyasi-Agyei and Willgoose* [1997, 1999], *Gyasi-Agyei* [1999, 2005], *Koutsoyiannis and Onof* [2001], *Molnar and Burlando* [2005], and *Gyasi-Agyei and Mahbub* [2007]. Recent reviews on the subject matter have been provided by *Beuchat et al*. [2011], *Gyasi-Agyei* [2011, 2012], and *Westra et al*. [2012]. *Beuchat et al*. [2011] included surface air temperature, relative humidity, mean sea level pressure, and wind speed in the list of predictors for estimating target subdaily statistics through multivariate adaptive regression required for downscaling daily rainfall data.

[6] Applications of copula theory are gaining strong grounds in hydrology with the establishment of the International Commission on Statistical Hydrology of the International Association of Hydrological Sciences (ICSH-IAHS) website (www.stahy.org) that keeps track of published papers. A copula offers a flexible way of mapping multidimensional uniform distributions to a single uniform distribution without regard to the marginal distributions. *Joe* [1997], *Nelson* [2006], and *Salvadori et al*. [2007] provide an introduction to copula modeling. Copula theory applications specific to rainfall modeling include *De Michele and Salvadori* [2003], *Palynchuk and Guo* [2011], *Zhang and Singh* [2007], *Kao and Govindaraju* [2008], and *Serinaldi and Grimaldi* [2007], with *Gyasi-Agyei and Melching* [2012] providing a recent review. *Gyasi-Agyei* [2011] and *Gyasi-Agyei and Melching* [2012] have adopted pair-copula construction [e.g., *Aas et al*., 2009] for modeling the joint distribution of three important characteristics of storm profiles. Pair-copula construction eases the computational burden of multidimensional modeling and also offers the flexibility of adapting different bivariate copulas for the linkages. Metaelliptic copulas [e.g., *Fang et al*., 2002] for modeling trivariate hydrologic data were introduced by *Genest et al*. [2007]. As noted by *Gyasi-Agyei and Melching* [2012], the computation of the square root of the covariance matrix via Cholesky decomposition in the simulation process of metaelliptic copulas does not allow the preservation of the quantile of the leading variable of the daily rainfall amount in the disaggregation process. This means the 3-D metaelliptic copulas will generate three different quantiles for each simulation run, defeating the purpose of preserving the numerical value of the daily rainfall amount.

[7] Despite the significant advances in the understanding of climate change, there still remains a knowledge gap in relation to the quantitative effects on fine timescale rainfall statistics. This is largely due to the inability of global climate models (GCMs) and regional climate models (RCMs) to downscale below daily or hourly timescales. This paper presents an enhanced version of the copula-based daily rainfall disaggregation model presented by *Gyasi-Agyei* [2011]. The model uses a pair-copula construction to capture the 3-D joint distribution of the total daily rainfall amount (R, mm), total wet periods' duration (L, h), and the maximum wet period's proportional depth (M).

[8] The novelties of this paper include the grouping of the site rainfall data using maximum daily temperature quantiles to reflect seasonal temperature shifts instead of the usual monthly grouping. This is supported by empirical evidence provided in this paper. Then, the daily rainfall disaggregation model parameters are explicitly conditioned on maximum daily temperature in order to allow capturing of seasonal temperature shifts. In this way, a quantitative assessment of the effects of temperature changes on fine timescale rainfall can be made. Using temperature classes improves the parameter estimation, as the number of wet days in the classes can be controlled unlike the monthly grouping where some dry months may not have sufficient rainfall events, particularly for tropical climates where rainfall is concentrated within the wet season of a few months. Calibration of the wet/dry (1/0) binary indicator submodel on the storm profile only, thus ignoring the leading and ending zeros of the 24 h day, is an additional enhancement that improves the performance of the model and also shortens the simulation time. Other enhancements are the incorporation of storm profile types that allows accurate modeling of consecutive wet days, and the expansion of the range of copulas (including metaelliptic) and marginal distributions types. Also, the total wet periods' duration, the maximum wet period proportional depth random variables, and the lag-1 autocorrelation statistics of the wet periods' depth are transformed to the positive real line to significantly improve the marginal distributions fitting by the maximum likelihood method.

[9] Figure 1 gives an overview of the variables considered in the modeling processes. A daily rainfall, starting at 9 A.M. of the previous day and ending at 9 A.M. on the measured day (24 h), as normally measured by conventional daily rain gauges, consists of three wet bursts of durations w_1, w_2, and w_3 summing up to the total wet periods' duration, L. The 10 sampling timescale wet periods' depths, r_i, of maximum r_{max}, sum up to the total daily rainfall amount R, and the maximum wet period proportional depth, M, is given as r_{max}/R. Two dry periods, d_1 and d_2,

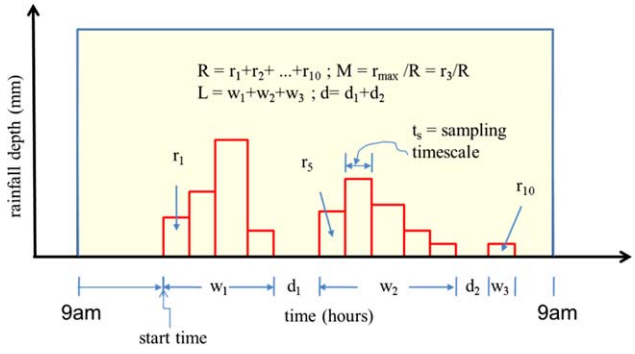

Figure 1. A definition sketch of daily rainfall and the disaggregated components.

Table 1. Six Minute and Long Records of Daily Rainfall Data Summary

Data Set ID	Capital City	Period From	Period To	Number of Wet Days	Mean (mm)	Variance (mm^2)
Six Minute Timescale						
1	SYD1	04/01/1913	28/08/1957	3987	11.9	312.7
2	SYD2	29/08/1957	15/05/2006	3988	12.6	354.1
3	DAR	02/11/1953	22/02/2006	3928	19.2	558.1
4	BNE	18/06/1949	14/02/2000	3720	12.7	410.4
Daily Timescale						
5	SYD	06/01/1859	23/12/2011	14,376	12.6	350.1
6	DAR	01/01/1945	31/12/2011	5970	18.8	578.6
7	BNE	02/01/1951	25/12/1999	2964	13.5	391.9

separate the wet bursts. The modeling effort is to distribute the measured daily total rainfall amount over the wet periods, as well as the determination of the start and end times within the 24 h period. Also important is the simulation of the dry periods within the wet bursts.

[10] This paper is organized as follows. First, the data used and the empirical evidence of the effects of temperature on the random variables *R*, *L*, and *M* of a storm profile are presented. This is followed by an overview of the copula-based daily rainfall disaggregation model. The next section is on the parameter identification of the submodels. Quantitative assessment of the effects of temperature changes on fine timescale rainfall statistics is next presented before the summary.

2. Data

[11] Rainfall records (daily and 6 min timescales) of three Australia capital cities located in different climatic regions are used in this paper (refer to *Gyasi-Agyei* [2012, Fig. 2] for an Australian map showing the location of the capital cities). Sydney, with an average annual rainfall of about 1200 mm, is located in a temperate region experiencing rainfall throughout the year, but heavy falls occur between January and June. Brisbane, situated in a subtropical region, has wet summers and dry winters with a mean annual rainfall of 1200 mm. Because of its tropical climate, Darwin's rainfall (mean annual amount of 1700 mm) occurs mostly between December and March, with little or no rainfall in June and July. Six minute timescale rainfall records were obtained from the Australia Bureau of Meteorology (BOM). The data date back to 1913 for Sydney (SYD), 1953 for Darwin (DAR), and 1949 for Brisbane (BNE). Sydney data, having a long record length, were split into two equal parts up to 28/8/1957 (SYD1) and after (SYD2), using SYD1 for parameter identification and SYD2 for model verification. This could not be done for the other two stations because of their relatively short record length. The 6 min rainfall data of 0.01 mm depth resolution are stored on a daily basis from midnight to midnight. Since the intention of this research is to disaggregate the long records of daily rainfall available freely online (http://www.bom.gov.au/climate/data/index.shtml) that are recorded from 9 A.M. to 9 A.M., the 6 min resolution data were processed to conform with the timings of the daily rainfall data, i.e., from 9 A.M. to 9 A.M. instead of from midnight to midnight. Records of total daily rainfall depth less than 1 mm or of 6 min duration were neglected as false events. Table 1 presents the daily rainfall data summary of the two timescales of records that also have maximum daily temperature records required for model parameterization and simulation.

[12] Another enhancement of the copula-based daily rainfall disaggregation model is the incorporation of storm profiles classified into four types (SP1, SP2, SP3, and SP4 as shown in Figure 2) based on the definitions of scale storm profiles (SSP1, SSP2, SSP3, SSP4) in *Gyasi-Agyei* [2012]. Table 2 provides the breakdown of the wet days into storm profile types. A very high proportion of the wet days are of type SP1, even within a cluster of wet days (SP1b).

[13] Since the prime objective of this paper is to evaluate the effects of temperature on the fine timescale rainfall, the minimum, mean, and maximum daily temperature within the last 24 h to 9 A.M. were investigated. The temperature (*T*, °C) data recorded to the nearest decimal were also obtained freely from the BOM website. While each of the three temperature statistics has a strong correlation with the daily rainfall random variables (*R*, *L*, *M*), the maximum daily temperature was found to be the best predictor. Additionally, maximum temperature boasts the longest records available. Up to 5 days lag before 9 A.M. were investigated,

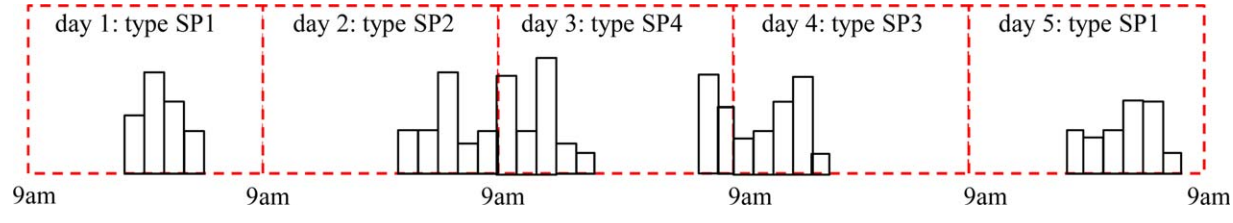

Figure 2. A definition sketch of the different daily storm profile types.

Table 2. Proportion of Storm Profile Types

Capital City	Isolated SP1a	Cluster of Wet Days SP1b	SP2	SP3	SP4
SYD1	0.284	0.468	0.113	0.113	0.021
SYD2	0.312	0.444	0.111	0.111	0.023
DAR	0.255	0.584	0.069	0.069	0.022
BNE	0.337	0.488	0.081	0.081	0.013

but the current day (within the last 24 h) value was the most influential. Figure 3 shows the variation of the maximum daily temperature statistics with the day of the year. Well-pronounced seasonality is depicted for Sydney and Brisbane, with little seasonal variation of temperature for Darwin as it is situated in a tropical region. Hereafter, temperature refers to the maximum daily temperature. Note that the discontinuities introduced as a result of rainfall and temperature data sampling were removed by adding a random jitter sampled from a uniform distribution RP $\sim U(-r_p, r_p)$ where r_p is half the data resolution, 0.005 mm for R, 0.05 h for L, and 0.05°C for T [*Gyasi-Agyei*, 2011, 2012; *Gyasi-Agyei and Melching*, 2012; *Vandenberghe et al*., 2010].

3. Empirical Evidence of Temperature Effects

[14] In order to assess the effects of temperature, the data were grouped into 16 temperature quantile classes defined by the probabilities {0.00,0.05,0.10,0.15,0.20,0.30,0.40, 0.50,0.60,0.70,0.75,0.80,0.85,0.90,0.94,0.97,1.00} instead of the traditional monthly grouping. One major disadvantage of the monthly classification of rainfall data is the likelihood of lack of rain in some months, particularly for Darwin. Also, the number of groups is limited to 12 for monthly grouping. For each temperature class, the 25th, 50th, 75th, 95th, 99th, and 100th (maximum) percentiles of the random variables modeled by the copula submodel were calculated and plotted against mean class temperature in Figure 4. The empirical data points demonstrate an exponential trend; therefore, an exponential regression (i.e., fitting a least squares linear regression to the logarithm of the quantiles [y] as $\ln[y] = c + \alpha T$) was performed and shown by the solid lines in Figure 4. The estimated exponential rates of change per 1°C rise in temperature (α) are presented in Table 3. It is observed that the exponential rate of change is quite consistent up to 75th percentile before reducing in numerical value with further increase in the percentile. Clearly, the random variable L shows an exponential decay with increasing temperature, while M demonstrates a strong exponential growth. For the random variable R, the tropical Darwin station shows a very strong decreasing trend, but the change is mild for Sydney and Brisbane. These observed rates of change are quite significant, particularly for the hot climate of Darwin where they are in excess of 15% for R and L for all percentiles, demonstrating a strong link between temperature and the storm profile quantiles.

Table 3. Exponential Rates of Change per 1°C Change in Temperature (%)

	Sydney			Darwin			Brisbane		
Percentile	R	L	M	R	L	M	R	L	M
25th	−2.2	−3.6	2.9	−15.7	−24.6	16.5	0.3	−4.3	4.2
50th	−2.4	−3.8	3.6	−18.6	−27.0	14.8	1.2	−3.9	3.8
75th	−2.7	−3.1	3.3	−17.6	−25.0	10.5	2.5	−4.2	3.2
95th	−1.2	−1.7	2.2	−16.3	−22.2	7.4	2.2	−3.3	2.0
99th	0.0	−0.9	1.5	−17.8	−19.2	4.8	2.5	−1.7	0.8
100th	−2.1	−0.6	1.2	−19.5	−12.5	2.8	−3.8	−1.0	1.0

[15] To assess whether the pair random variables (R-L, R-M, and L-M) of the two Sydney data sets of the same temperature class are from the same distribution, the D test statistic for the two-sample 2-D Kolmogrov-Smirnov (KS) test [*Press et al*., 2007] was performed. Note that the Sydney data were split into two equal halves of wet days after grouping the data into the 16 temperature classes. Hence, the number of wet days within the same temperature class could be different for the data sets. Table 4 provides the 2-D KS test p values with mean class values of 0.26, 0.33, and 0.24 for R, L, and M, respectively. Therefore, the assumption that the random variables within the same temperature class came from the same distribution cannot be rejected at the 1% significance level. This implies that the parameters calibrated with one half of the data set can be safely used for the other half and also for data collected in

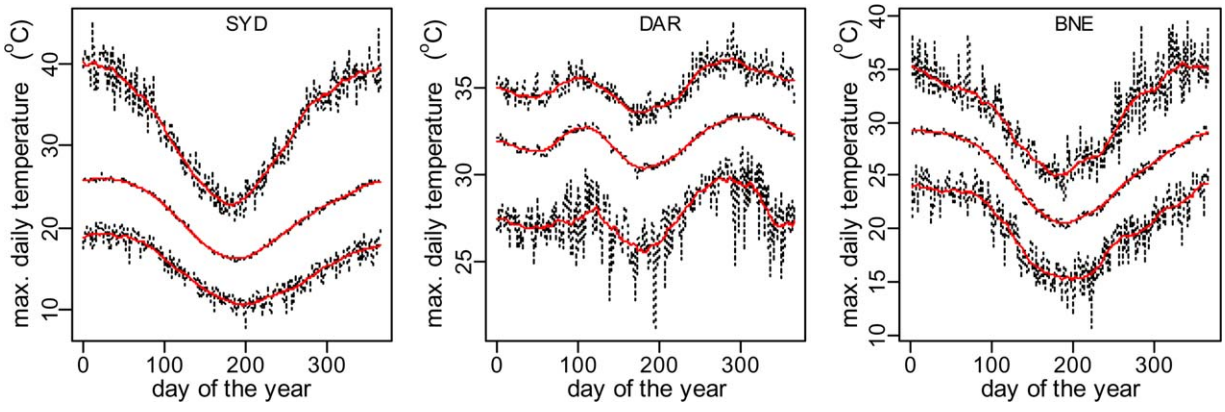

Figure 3. Variation of maximum daily temperature of all available full year records: dashed lines: upper is the maximum, middle is the mean, and lower is the minimum for the day of the year, and the red solid lines are the 30 day centered moving average.

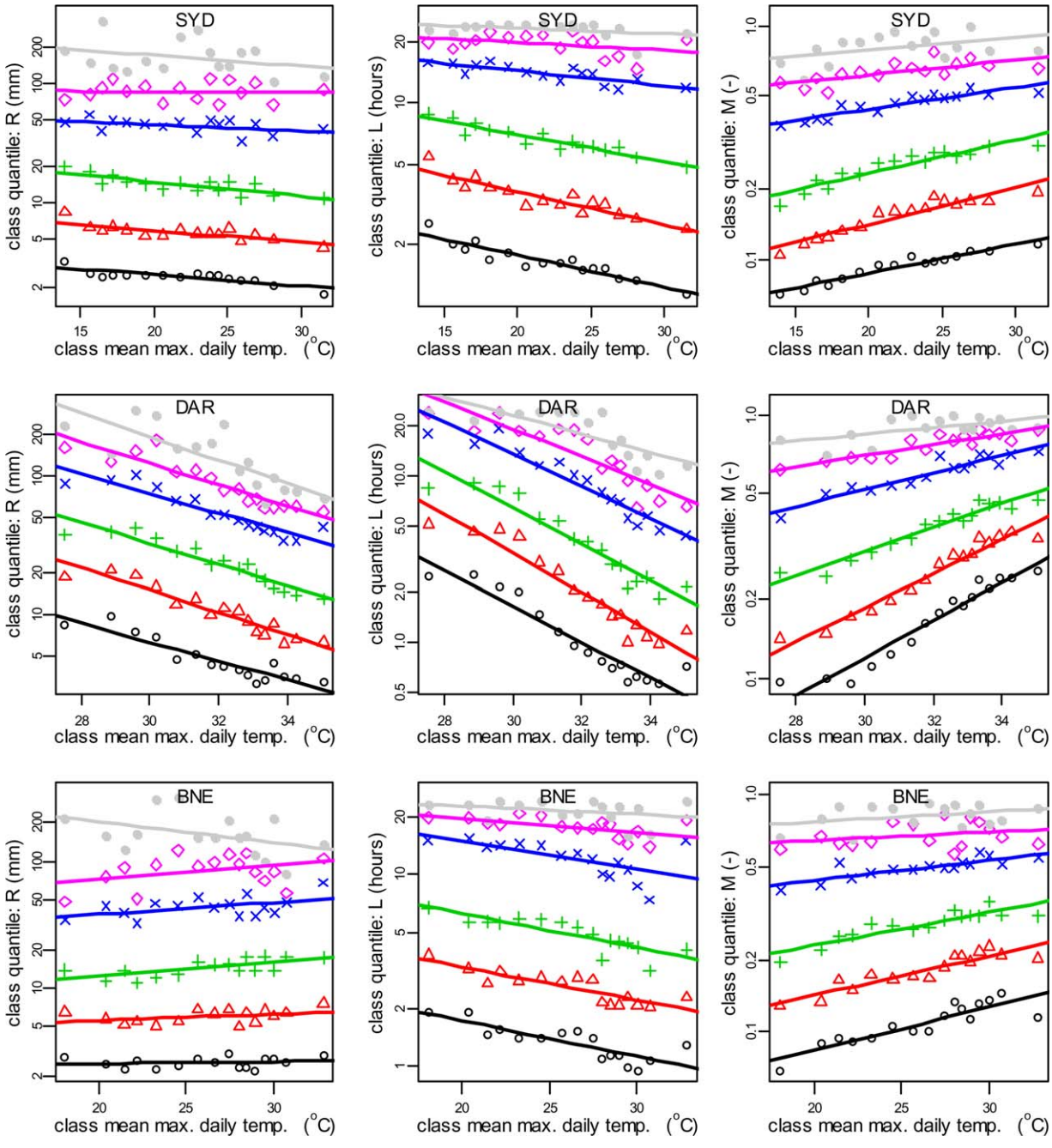

Figure 4. Variation of observed 25th (bottom, black), 50th, 75th, 95th, 99th, and 100th (top, brown) percentiles of the random variables with class mean temperature (symbols) and the exponential regression fitted (solid lines): daily amount (R), total wet periods' duration (L), and maximum wet period proportional depth (M).

the future. With respect to the individual random variables within the same temperature class, 1-D KS and Mann-Whitney-Wilcoxon tests were performed, and the results were consistent with the 2-D KS test.

[16] The 2-D KS test was also used to ascertain whether within the same site data set, the distributions of the random variables of the different temperature classes are different. An example 2-D KS test p values comparing R-L pair random variables within the different temperature classes is presented in Table 5 for Darwin. The mean 2-D KS test p values and the temperature change along the diagonals, parallel to the principal diagonal which runs from top left to bottom right in Table 5, that signify the same number of temperature classes apart were computed and presented in Table 6 for Sydney and Darwin. Darwin has the smallest temperature range, but the random variables are the most sensitive to temperature changes. It is clear that a small change in temperature could cause the

Table 4. The 2-D KS Test *p* Values for Comparing Pair Random Variables Within the Same Temperature Class of the Two Data Sets for Sydney

Temperature Class	Number of Wet Days		Pair Random Variables		
	SYD1	SYD2	*R-L*	*R-M*	*L-M*
1	285	114	0.339	0.387	0.766
2	236	163	0.674	0.947	0.658
3	238	161	0.000	0.000	0.090
4	208	190	0.136	0.151	0.240
5	395	403	0.339	0.269	0.201
6	399	398	0.035	0.144	0.003
7	417	381	0.406	0.444	0.072
8	391	406	0.051	0.514	0.200
9	381	416	0.004	0.265	0.013
10	161	238	0.376	0.353	0.526
11	202	197	0.197	0.126	0.041
12	161	237	0.001	0.023	0.000
13	187	212	0.017	0.044	0.004
14	128	191	0.818	0.633	0.306
15	97	142	0.551	0.765	0.601
16	101	139	0.208	0.164	0.084

distribution of the random variables to change significantly, particularly in the tropics, necessitating investigation of varying distributional parameters across the temperature classes.

4. The Copula-Based Daily Rainfall Disaggregation Model

[17] The joint distribution of the three important random variables (*R*, *L*, and *M*) of a storm profile is modeled by 3-D copulas through pair-copula construction to ease computational demands. The pair-copula construction [*Bedford and Cooke*, 2001, 2002; *Aas et al*., 2009] is based on a vine which is a cascade tree structure constructed for modeling the dependence of random variables. *Gyasi-Agyei* [2011] adopted the drawable vine (D-vine) for modeling the dependence of the random variables because of the strong correlation between the *R-L* (positive) and *L-M* (negative) pairs but a weaker negative correlation between the *R-M* pair.

[18] Based on Sklar's theorem and the chain rule of *Joe* [1996], a D-vine has the 2-D ($F_{2|1}$) and 3-D ($F_{3|12}$) marginal conditional distributions given as

$$F_{2|1}(x_2|x_1) = \frac{\delta C_{12}\{F_1(x_1), F_2(x_2); \theta_{12}\}}{\delta F_1(x_1)}$$
$$F_{3|12}(x_3|x_1, x_2) = \frac{\delta C_{13|2}\{F_{3|2}(x_3|x_2; \theta_{23}), F_{2|1}(x_2|x_1; \theta_{12}); \theta_{13|2}\}}{\delta F_{2|1}(x_2|x_1)} \quad (1)$$

where $F_i(x_i)$ is the univariate continuous marginal distribution function of random variable X_i, C_{ij} is the bivariate linking copula for random variables X_i and X_j with the associated parameter θ_{ij}, and parameter $\theta_{13;2}$ is the conditional dependent of the first and third univariate margins given the second. Equation (1) is termed the *h*-function, written as $h(u_i,u_j,\theta_{ij}) = F_{i|j}(x_i|x_j)$, with $u_i = F_i(x_i)$, and the partial derivative is taken with respect to the second variable. The derivation of the conditional distribution *h*-functions has been highlighted by *Gyasi-Agyei and Melching* [2012]. In the context of this paper, the random variables are assigned as $R = X_1$, $L = X_2$, and $M = X_3$. Sampling of the random variable *L* from a bivariate copula for a given value of *R* and daily temperature (*T*) is the starting point, after which *M* is sampled from a different bivariate copula conditioned on *T*, *R*, and the sampled *L* values.

[19] For a storm profile of total wet periods' duration of *L* (h), the number of wet periods, n_L, is defined as the integer of $L/t_s + 0.5$, t_s being the simulation timescale. Defining $z_i = \ln(r_i)$ where r_i are the wet period depths, a first-order autoregressive lognormal submodel defined as

$$z_i - \mu_Z = \rho(z_{i-1} - \mu_Z) + e_i \quad (2)$$

is used to model z_i, and therefore r_i, to distribute *R* over the n_L wet periods. In equation (2), μ_Z is the mean and ρ is the lag-1 autocorrelation coefficient of z_i with values within ± 1. The white noise e_i is normally distributed as $N(0, \sigma_E^2)$

Table 5. The 2-D KS Test *p* Values Comparing Random Variable Pair *R-L* Within Different Temperature Classes of the Darwin Data Set

Class	1	2	3	4	5	6	7	8	9	10	11	12	13	14	15	16
Mean *T* (°C)	27.5	28.9	29.6	30.2	30.8	31.3	31.8	32.2	32.6	32.9	33.1	33.4	33.6	33.9	34.3	35.1
1	1.00	0.52	0.73	0.60	0.00	0.00	0.00	0.00	0.00	0.00	0.00	0.00	0.00	0.00	0.00	0.00
2	0.52	1.00	0.65	0.33	0.00	0.00	0.00	0.00	0.00	0.00	0.00	0.00	0.00	0.00	0.00	0.00
3	0.73	0.65	1.00	0.38	0.00	0.00	0.00	0.00	0.00	0.00	0.00	0.00	0.00	0.00	0.00	0.00
4	0.60	0.33	0.38	1.00	0.00	0.00	0.00	0.00	0.00	0.00	0.00	0.00	0.00	0.00	0.00	0.00
5	0.00	0.00	0.00	0.00	1.00	0.35	0.00	0.00	0.00	0.00	0.00	0.00	0.00	0.00	0.00	0.00
6	0.00	0.00	0.00	0.00	0.35	1.00	0.05	0.01	0.00	0.00	0.00	0.00	0.00	0.00	0.00	0.00
7	0.00	0.00	0.00	0.00	0.00	0.05	1.00	0.14	0.15	0.03	0.00	0.00	0.00	0.00	0.00	0.00
8	0.00	0.00	0.00	0.00	0.00	0.01	0.14	1.00	0.80	0.29	0.09	0.00	0.00	0.00	0.00	0.00
9	0.00	0.00	0.00	0.00	0.00	0.00	0.15	0.80	1.00	0.62	0.34	0.00	0.00	0.00	0.00	0.00
10	0.00	0.00	0.00	0.00	0.00	0.00	0.03	0.29	0.62	1.00	0.88	0.06	0.05	0.05	0.01	0.02
11	0.00	0.00	0.00	0.00	0.00	0.00	0.00	0.09	0.34	0.88	1.00	0.10	0.01	0.30	0.03	0.19
12	0.00	0.00	0.00	0.00	0.00	0.00	0.00	0.00	0.00	0.06	0.10	1.00	0.49	0.22	0.81	0.46
13	0.00	0.00	0.00	0.00	0.00	0.00	0.00	0.00	0.00	0.05	0.01	0.49	1.00	0.00	0.04	0.17
14	0.00	0.00	0.00	0.00	0.00	0.00	0.00	0.00	0.00	0.05	0.30	0.22	0.00	1.00	0.33	0.57
15	0.00	0.00	0.00	0.00	0.00	0.00	0.00	0.00	0.00	0.01	0.03	0.81	0.04	0.33	1.00	0.39
16	0.00	0.00	0.00	0.00	0.00	0.00	0.00	0.00	0.00	0.02	0.19	0.46	0.17	0.57	0.39	1.00

Table 6. Average 2-D KS Test p Values Comparing Pair Random Variables at a Number of Temperature Classes Apart (Along the Diagonals Parallel to the Principal, e.g., of Table 5) Within the Same Data Set[a]

Number of Classes Apart	SYD1				DAR			
	ΔT (°C)	*R-L*	*R-M*	*L-M*	ΔT (°C)	*R-L*	*R-M*	*L-M*
0	0.00	1.000	1.000	1.000	0.00	1.000	1.000	1.000
1	1.17	0.238	0.309	0.227	0.50	0.379	0.432	0.391
2	2.15	0.265	0.209	0.184	0.92	0.196	0.139	0.181
3	3.12	0.379	0.230	0.180	1.33	0.158	0.092	0.116
4	4.11	0.219	0.170	0.145	1.72	0.045	0.090	0.019
5	5.12	0.088	0.073	0.087	2.11	0.019	0.014	0.004
6	6.13	0.165	0.100	0.119	2.50	0.002	0.002	0.000
7	7.17	0.089	0.072	0.067	2.90	0.000	0.000	0.000
8	8.21	0.083	0.037	0.027	3.32	0.000	0.000	0.000
9	9.21	0.025	0.003	0.004	3.73	0.000	0.000	0.000
10	10.22	0.016	0.004	0.000	4.17	0.000	0.000	0.000
11	11.25	0.008	0.001	0.005	4.65	0.000	0.000	0.000
12	12.32	0.012	0.001	0.000	5.17	0.000	0.000	0.000
13	13.51	0.001	0.000	0.000	5.75	0.000	0.000	0.000
14	15.04	0.000	0.000	0.000	6.47	0.000	0.000	0.000
15	17.56	0.000	0.000	0.000	7.53	0.000	0.000	0.000

[a] ΔT is the mean temperature difference.

with a mean value of zero and a variance of $\sigma_E^2 = (1-\rho^2)\sigma_Z^2$. Invoking the basic properties of the lognormal distribution, $\mu_Z = \ln(R/n_L) - \sigma_Z^2/2$, noting that the statistics μ_Z and σ_Z are different for each wet day and are obtained from knowledge of the statistics ρ and σ_E which are dependent on the random variables R, L, and M obtained from the copula submodel.

[20] The four-parameter nonrandomized Bartlett-Lewis (BL) model [*Rodriguez-Iturbe et al*., 1987; *Gyasi-Agyei*, 2011] is used to generate the indicator function of a wet/dry (1/0) binary sequence defining the storm profile. An improvement of the disaggregation model in this paper is the calibration of the BL model parameters only on the storm profile (from the beginning to the end of rain) rather than the 24 h duration. The simulated storm profile of duration D (h) is then shifted to the desired location within the wet day depending on the storm profile type as discussed later on. This approach improves the performance of the BL model and also shortens the simulation time. The four parameters of the binary chain submodel to be calibrated are defined as

[21] (1) λ (h^{-1}): the rate parameter of the Poisson process governing storm arrivals;

[22] (2) β (h^{-1}): the Poisson process rate parameter governing the cell arrivals associated with storm origins;

[23] (3) η (h^{-1}): the exponential distribution rate parameter of the duration of the rectangular pulse associated with each cell; and

[24] (4) γ (h^{-1}): the rate parameter of the exponential distribution of storm duration.

5. Parameter Identification and Linkage With Temperature

5.1. Copula

[25] Following *Gyasi-Agyei and Melching* [2012], 6 two-parameter (shape and scale) distributions were considered for the marginal distributions of the random variables R, M, and L. They are gamma (GA), Weibull (WE), lognormal (LN), Kappa (KA), log-logistic (LL), and generalized Pareto (GP) distributions. The random variables L and M were transformed to the positive real line as $L_T = L/(24.1 - L)$ and $M_T = M/(1 - M)$ and the marginal distributions fitted to L_T and M_T, before transforming back to the quantiles using the inverse relationships $L = 24.1 \times L_T/(1 + L_T)$ and $M = M_T/(1 + M_T)$. These transformations led to a better fitting of the marginal distributions. A common marginal distribution and bivariate copula were sought for each rainfall station. The parameters were initially estimated independently for each T class by the maximum likelihood method, and the results were plotted for identification of the best polynomial curve fit with mean class T as the independent variable in order to reduce the number of parameters. It was observed that the shape and scale parameters are better predicted with log10(T) rather than T, and the first-order polynomial (par $= a_1 + b_1$ log10[T]) was adequate for the shape parameters as was the second order (par $= a_2 + b_2$ log10[T] $+ c_2$ log10[T]^2) for the scale parameters. The five polynomial coefficients (a_1, b_1, a_2, b_2, c_2) were estimated by jointly maximizing the sum of the log-likelihoods of the distribution for all the T classes, and the best distribution selected is the one with the highest Anderson-Darling (AD) class mean p value obtained using the fitted polynomial functions. While the number of fitted polynomial coefficients may seem many, 32 shape and scale parameters are being replaced with 5 for each of the R, L, and M random variables, a considerable reduction in the number of model parameters.

[26] Table 7 gives the best marginal distributions selected for the random variables with their calibrated parameter values of the fitted polynomial functions, and the T class mean AD p values determined using the fitted polynomial functions for the shape and scale parameters. For each T class, the shape parameter is set to the polynomial derived function of the five-coefficient calibration, and then the scale parameter is optimized independently. These class scale parameters are then fitted to derive the three coefficients of the scale polynomial function, and the resulting

Table 7. Marginal Distributions Selected and Their Calibrated Parameters

Random Variable	Distribution	Shape		Scale				*p* Value		
		a_1	b_1	a_2	b_2	c_2	R^2	Mean	N01	N05
SYD1										
R	WE	0.942	−0.206	31.62	−22.64	3.599	0.653	0.302	1	3
L_T	LL	0.890	−0.180	2.623	−4.364	0.741	0.897	0.319	0	3
M_T	LN	0.379	0.390	−8.496	8.431	−2.438	0.964	0.414	0	0
DAR										
R	WE	2.180	−0.885	−455.7	846.0	−353.9	0.909	0.340	0	4
L_T	LL	4.905	−2.825	−94.26	144.2	−55.24	0.931	0.197	4	6
M_T	LL	0.884	−0.263	76.71	−118.0	44.079	0.962	0.326	0	4
BNE										
R	WE	0.723	−0.028	196.5	−282.3	105.7	0.461	0.298	0	0
L_T	LL	0.963	−0.208	0.477	−1.034	−0.541	0.781	0.283	0	1
M_T	LL	0.600	−0.060	−13.99	15.28	−4.558	0.879	0.458	1	1

coefficient of determination (R^2) is shown in Table 7. The high R^2 values indicate a very good fit of the polynomial functions, with the exception of the random variable R for Brisbane. A lower R^2 value indicates a near-constant parameter value over the T classes. Also indicated are the number of T classes out of 16 that failed at the 1% (N01) and 5% (N05) significance levels. In general, the fit was good for all random variables except for L for Darwin which had four T classes failing at the 1% significance level. Note that the Weibull distribution emerged as the best for R and so did the log-logistic distribution for both L_T and M_T.

[27] Figure 5 shows examples of pair scatterplots and bivariate empirical copulas of the random variables for selected temperature classes for SYD1 and DAR data sets to give an insight into the type of relationship between the random variables. The best copula models were selected from the 11 bivariate copulas described in detail by *Gyasi-Agyei and Melching* [2012]:

[28] (1) M1: the Moran-Downton bivariate exponential (only for positive dependence);

[29] (2) M2: the bivariate Fisher (only for positive dependence);

[30] (3) M3: the metaelliptic bivariate Pearson type II;

[31] (4) M4: the metaelliptic Normal;

[32] (5) M5: the metaelliptic Cauchy;

[33] (6) M6: the metaelliptic Student t with 5 degrees of freedom;

[34] (7) M7: the metaelliptic Student t with 10 degrees of freedom;

[35] (8) M8: Clayton (only for positive dependence);

[36] (9) M9: Frank;

[37] (10) M10: Gumbel-Hougaard (only for positive dependence); and

[38] (11) M11: Plackett.

[39] The parametric bootstrap method of *Genest et al.* [2007] was used to select the appropriate bivariate copula. It is based on the Cramer-von Mises Sn statistic, and the p values were estimated by setting the number of iterations to 1000, and using the maximum likelihood method to estimate the parameters. Algorithms for the 3-D pair-copula parameter estimation and simulation are summarized by *Gyasi-Agyei* [2011].

[40] Here too the number of copula model parameters was reduced considerably by applying a first-order polynomial ($\text{par} = a_3 + b_3 \log10[T]$) and estimating the coefficients by maximizing the sum of the log-likelihoods of the copulas for all T classes. Figure 6 depicts the estimated copula parameters and the fitted polynomial function for Sydney (SYD1), and Table 8 shows the selected copulas and their calibrated polynomial coefficient values for the three capital cities. Note that the polynomial functions fitted for the marginals were used to generate the probabilities before fitting the first tree copulas. The same was done to the first tree copula parameters to generate the second tree probability vectors before fitting the copulas. A very low value of R^2 close to 0 indicates that a constant value would be appropriate in lieu of the polynomial function. The main indicators of acceptance of the copulas are the mean T class p values, and also N01 and N05 values which indicate only a few T classes did not pass at the 1% significance level.

5.2. Dry Probability Submodel

[41] In order to estimate the dry probability submodel parameters, each wet day storm profile (i.e., ignoring the leading and ending zeros of the 24 h duration) was aggregated individually at levels contained in h_j {1,2,3,4, 5,6,7,8,9,10, 15,20,25,30,35,40,45,50,55,60} where h_j times the simulation timescale (t_s) of 6 min gives the aggregation timescale. For each storm profile, only a few of the aggregation levels listed are considered appropriate. As a matter of fact, this includes only those aggregation levels that produce an integer greater than two for the ratio $m_i = D_n/h_i$, where D_n is the number of data points of the storm profile which upon multiplication with t_s gives the duration of the storm profile (D, h). Also, for m_i values of one or two, it is obvious that $P(h) = 0$ and they are not included in the parameter estimation. This integer consideration avoids the problem of an unequal number of data points within aggregation intervals. While *Gyasi-Agyei and Melching* [2012] used a similar approach for storm events, they fitted a different dry probability submodel. The approach adopted herein for estimating the dry probability parameters improves the fitting and speeds up the simulation process. As an example calculation, take a wet/dry (1/0) binary storm profile of {1,1,0,1,1, 1,0,0,0,1} of the simulation timescale having $D_n = 10$, $D = 10 \times 0.1 = 1$ h for which

[42] (1) $h_1 = 1$, $m_1 = 10/1 = 10$: the storm profile is the same as the $t_s = 6$ min of {1,1,0,1,1,1,0,0,0,1}, $P_{h=0.1} = 4/10$, is considered;

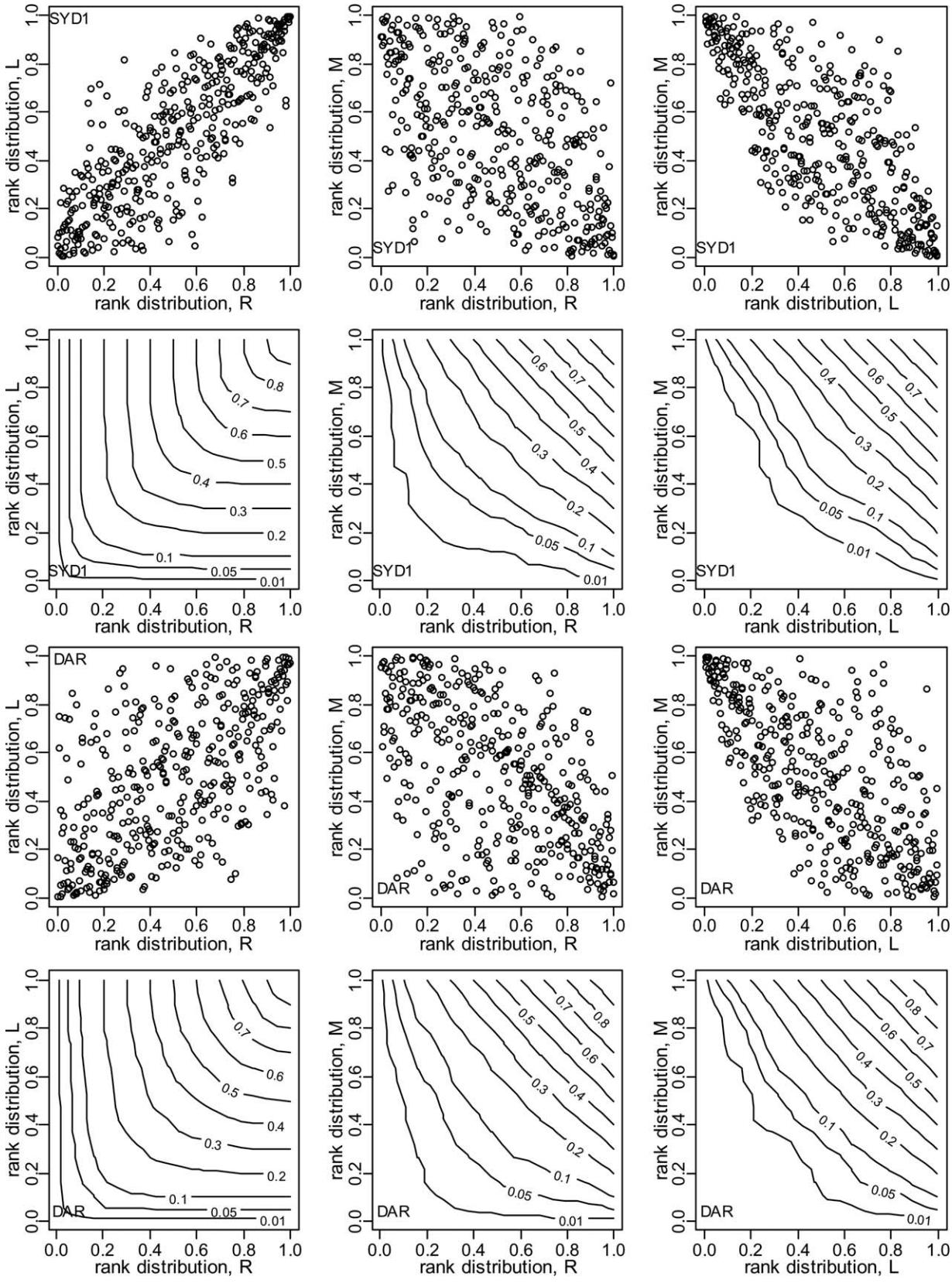

Figure 5. Example pair scatterplots of the bivariate rank distribution and contour levels of the empirical copula: SYD1 is for temperature class 6 of mean value 19.4°C, DAR is for temperature class 5 of mean value 30.8°C.

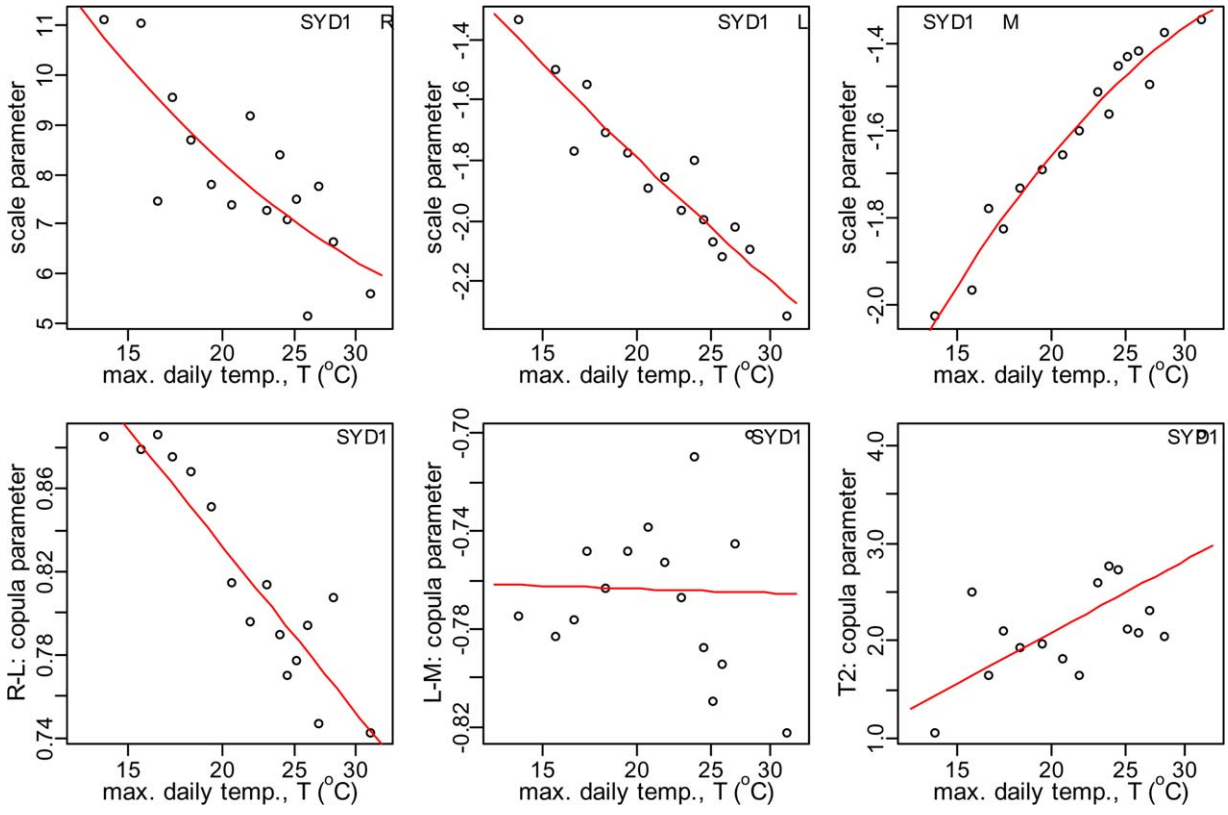

Figure 6. Calibrated marginal and copula model parameters for Sydney (SDY1): circles are the observed T class values and solid lines are the fitted. For the observed marginal parameters, the shape parameter was defined by the fitted polynomial and the scale parameters estimated for each class, and presented as circles.

[43] (2) $h_2 = 2$, $m_2 = 10/2 = 5$: the storm profile {(1,1),(0,1),(1,1),(0,0),(0,1)} is aggregated to the $t_s = 12$ min storm profile as {1,1,1,0,1}, $P_{h=0.2}$=1/5, is considered;

[44] (3) $h_3 = 3$, $m_3 = 10/3$: the storm profile {(1,1,0), (1,1,1),(0,0,0),(1,–,–)} is aggregated to $t_s = 18$ min storm profile as {1,1,0,–} is not considered because of the insufficient number of data points in the last aggregation interval; and similarly,

[45] (4) $h_4 = 4$, $m_4 = 10/4$: the storm profile {(1,1,0,1), (1,1,0,0),(0,1,–,–)} is aggregated to $t_s = 24$ min storm profile as {1,1,–} is not considered.

[46] There was no need to group the data into classes of any random variable. Therefore, for each station the mean of the dry probabilities of the aggregation levels was used to estimate the parameters as depicted in Figure 7. Table 9 provides the calibrated parameters for each capital city.

Table 8. Copula Models Selected and Their Calibrated Parameters

Pair Random Variables	Copula	Parameters			p Value		
		a_3	b_3	R^2	Mean	N01	N05
SYD1							
R-L	M1	1.421	−0.452	0.858	0.225	1	3
L-M	M6	−0.751	−0.010	0.001	0.357	0	2
T2	M11	−3.361	4.186	0.397	0.459	0	0
DAR							
R-L	M4	3.606	−2.011	0.717	0.437	0	0
L-M	M3	−1.031	0.253	0.013	0.157	2	7
T2	M11	1.137	−0.346	0.007	0.350	1	4
BNE							
R-L	M2	−35.67	36.10	0.730	0.400	0	2
L-M	M6	−0.934	0.117	0.083	0.205	0	2
T2	M11	1.166	−0.089	0.001	0.306	1	3

5.3. Transition Probability Defining Storm Profile Type

[47] The type of storm profile needs to be assigned to every wet day during the simulation. Other than SP1 types that are obvious, a methodology is required to determine the other storm types within a cluster of consecutive wet days. As seen in Table 2, SP1 dominates the data set as the possibility of rainfall crossing to the next day (past 9 A.M.) has been significantly reduced by processing the data for the wet days to run from 9 A.M. to 9 A.M. By their definitions, SP2 is the main trigger for a SP3 or SP4 to occur within a cluster of wet days, and also, only SP1 or SP2 can begin a pair of consecutive wet days. Hence, all that is required is to establish the probability of a SP2 beginning a pair of consecutive wet days as well as the transition probability from a SP2 to SP3. Another important thing to note is that the storm profile type at the end of a wet cluster is predefined depending on the last but one type, i.e., if the last but one is a SP2 or SP4, then the last will be a SP3, and if

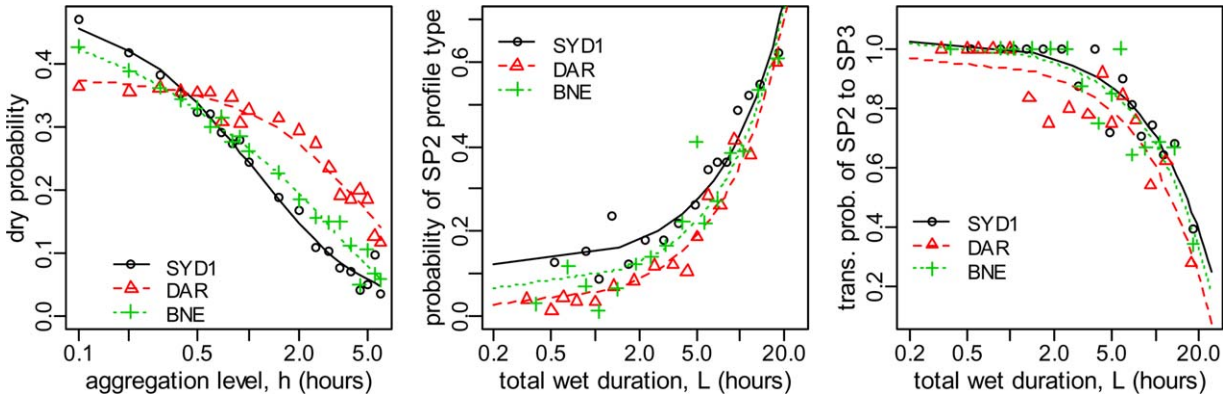

Figure 7. (left) Dry probability of storm profiles versus aggregation level, (middle) probability of a SP2 storm profile beginning a pair of consecutive wet days, and (right) the transition probability from a SP2 storm profile to a SP3 as a function of the total wet periods' duration, L (points are the observed values and solid lines are the fitted).

the last but one is a SP3 or SP1, then the last will be a SP1. It is observed that the probabilities are dependent on L, so 16 L quantile classes, defined by the same probability set used to define the T classes, were used to establish the relationship depicted in Figure 7 (middle and right). In order to reduce the number of parameters, the data points were fitted with a linear model ($\text{par} = a_4 + b_4 L$), and the calibrated coefficients (a_4 and b_4) are given in Table 9. The significantly high values of R^2 in Table 9 suggest that the fits are very good.

5.4. The Depth Process Submodel

[48] The parameters of the depth process submodel to be estimated are the lag-1 autocorrelation, ρ, and the white noise standard deviation, σ_E, related to equation (2). It was observed that the first statistic is dependent on L and the second on the product of R and M which gives the maximum wet period depth as reported by *Gyasi-Agyei* [2011] and *Gyasi-Agyei and Melching* [2012]. However, they exhibit a high random variability around the copula derived random variables that are captured by distributional fitting. The ρ statistic was transformed to the positive real line as $\rho_T = (1-\rho)/(1+\rho)$ before fitting the distributions, and then transformed back using the inverse relationship $\rho = (1-\rho_T)/(1+\rho_T)$. These two statistics were estimated for each wet day and the data grouped into L quantile classes for ρ and $R \times M$ quantile classes for σ_E. The same procedure used for selecting marginal distributions and the quantile class probabilities for fitting the copula submodel was adopted. However, a first-degree polynomial ($\text{par} = a_5 + b_5 x$) was fitted to the shape parameters, and a third degree ($\text{par} = a_6 + b_6 x + c_6 x^2 + d_6 x^3$) to the scale parameters in order to achieve acceptable AD p values. Note that the predictor x here is $\log10(L)$ for the statistic ρ_T and $\log10(R \times M)$ for σ_E. Figure 8 shows the fitted polynomials, and Table 10 gives the estimated parameters. As judged by the R^2 values, the polynomial fit was excellent, and the average AD class p values are quite high and acceptable. Only 2 classes failed at the 1% significance level and 11 at the 5% significance level out of the 96 (16×6) classes of the three rainfall stations. It needs to be underlined that the log-logistic distribution emerged as the best for both ρ_T and σ_E statistics.

Table 9. Dry Probability and Transition Probability Submodels' Calibrated Parameters

	Dry Probability			
Capital City	λ (h^{-1})	β (h^{-1})	γ (h^{-1})	η (h^{-1})
SYD1	0.122	0.361	0.046	1.334
DAR	0.163	0.010	0.260	0.173
BNE	0.294	2.277	0.300	2.179
	Transition Probability			
	Coefficient			
Capital City	a_4		b_4	R^2
T2				
SYD1	0.119		0.031	0.93
DAR	0.019		0.034	0.96
BNE	0.061		0.033	0.89
T2 to T3				
SYD1	1.032		−0.033	0.88
DAR	0.976		−0.037	0.84
BNE	1.027		−0.035	0.83

6. Effects of Temperature Changes

[49] The effects of temperature changes on fine timescale rainfall statistics is evaluated through an ensemble simulation using the presented improved copula-based daily rainfall disaggregation model. Below are the simulation steps followed:

[50] (1) for a given daily rainfall amount R (mm), measured at 9 A.M., the maximum daily temperature T(°C) within 24 h prior to 9 A.M. is used to determine the copula submodel parameters;

[51] (2) the copula submodel is then used to generate the total wet periods' duration L (h) and the maximum wet period proportional depth M;

[52] (3) the number of wet periods n_L is estimated as the integer of $L/t_s + 0.5$, where t_s (h) is the simulation timescale, which is 0.1 h for the case study data;

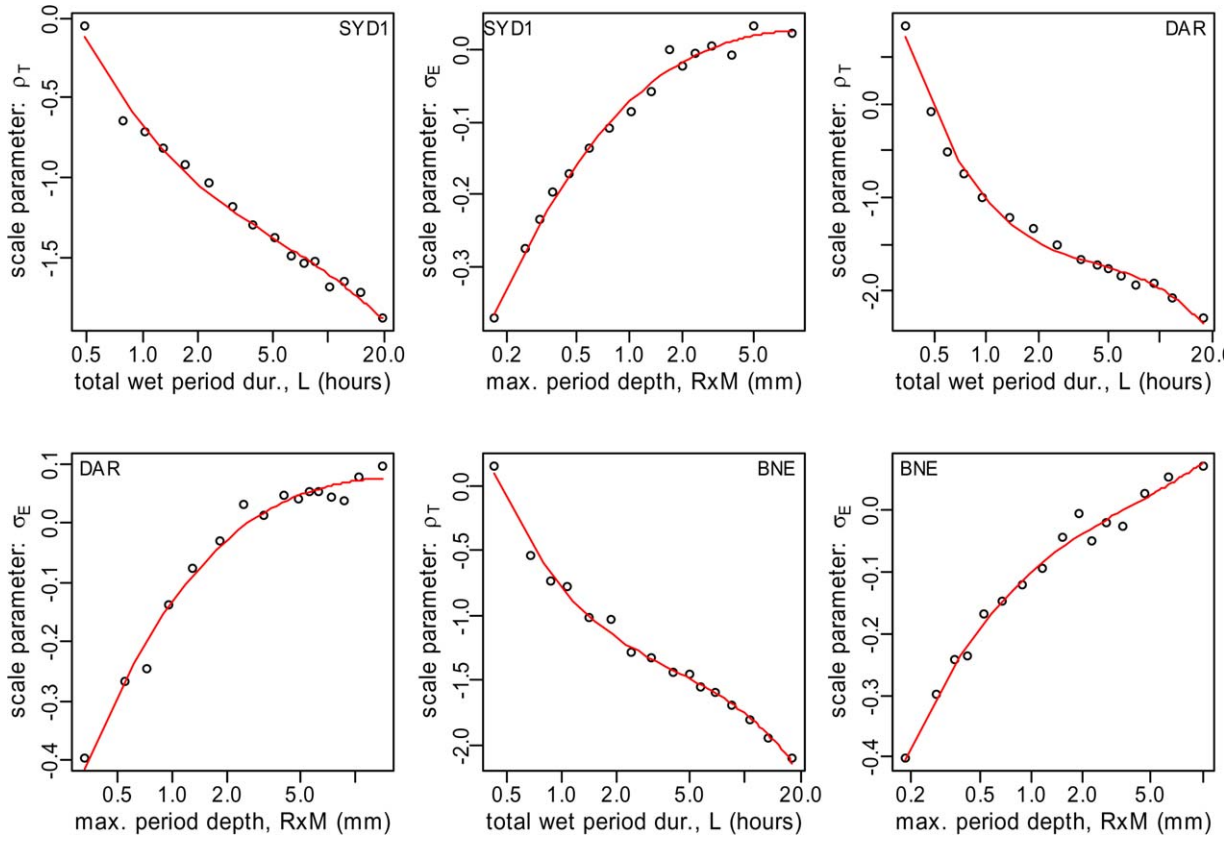

Figure 8. The depth process parameters: variation of transformed lag-1 autocorrelation (ρ_T) scale parameter with total wet periods' duration (L) and the standard deviation (σ_E) scale parameter with maximum wet period depth ($R \times M$) (circles are the observed values and solid lines are the fitted). The shape parameter was defined by the fitted polynomial and the scale parameters estimated for each class and presented as circles.

[53] (4) the Bartlett-Lewis submodel is activated to simulate a 1/0 binary sequence having exactly n_L 1s for the wet periods, the beginning and ending values being 1, and the total number of 1s and 0s times t_s gives the duration of the storm profile, D (h);

[54] (5) R, L, and M quantiles are used to estimate the depth process submodel parameters;

[55] (6) n_L wet period depths (r_i) are repeatedly generated until $\sum_{i=1}^{n_L} r_i$ is within a set limit of 5% of R, before applying proportional adjustment to achieve the equality $\sum_{i=1}^{n_L} r_i = R$;

[56] (7) the generated series of r_i is accepted if $r_{\max}/R$ is within a set limit of 5% of M, $r_{\max}$ being the maximum value of r_i;

[57] (8) quantile L is used to estimate the parameters of the SP2 and SP2 to SP3 transition probabilities which are used to assign a storm profile type;

[58] (9) if the storm profile type is SP1, then the start of the storm profile is drawn from a uniform distribution defined by the available time $\sim U(9\text{ A.M.}, [9\text{ A.M.} + 24 - D])$; and

[59] (10) for SP2, SP3, and SP4, the start times are predefined as explained earlier.

[60] Two daily rainfall time series, those derived from the 6 min data sets and the long records available at the

Table 10. Selected Marginal Distributions and Their Calibrated Parameters for the Depth Process Submodel

		Shape		Scale					p Value		
Capital City	Distribution	a_5	b_5	a_6	b_6	c_6	d_6	R^2	Mean	N01	N05
ρ_T											
SYD1	LL	0.456	−0.157	−0.650	−1.473	0.893	−0.382	0.99	0.343	2	2
DAR	LN	0.924	−0.226	−0.989	−2.141	2.364	−1.217	0.99	0.336	0	3
BNE	LL	0.512	−0.149	−0.781	−1.656	1.470	−0.797	0.99	0.549	0	2
σ_E											
SYD1	LL	0.128	0.002	−0.075	0.230	−0.165	0.041	0.99	0.434	0	0
DAR	LL	0.177	−0.039	−0.124	0.433	−0.323	0.082	0.98	0.448	0	2
BNE	LL	0.150	−0.004	−0.099	0.244	−0.161	0.091	0.99	0.329	0	2

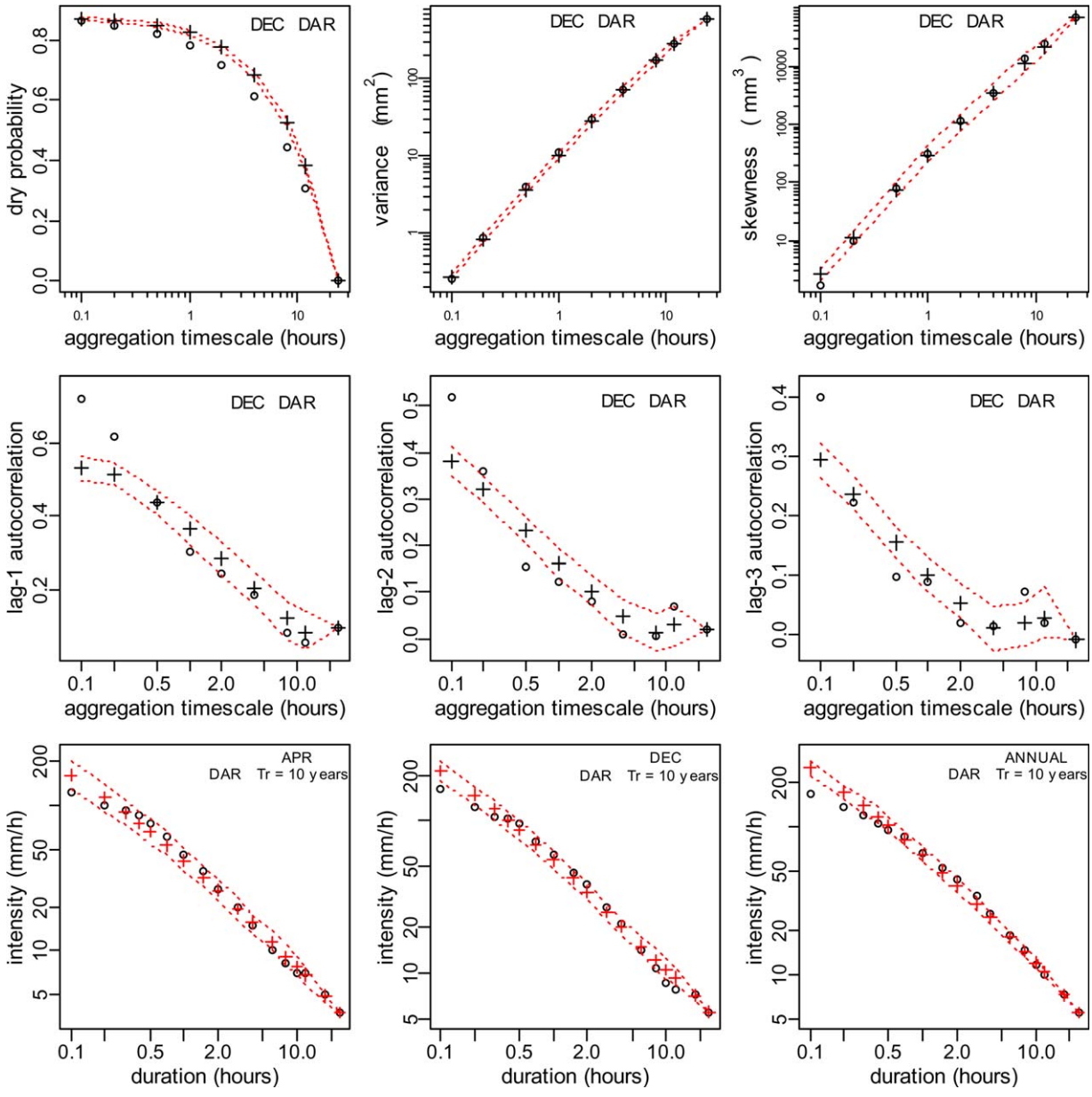

Figure 9. Comparison of the observed and simulated aggregation statistics and the intensity-duration-frequency (IDF) curves for Darwin (circles are the observed values, pluses are the simulated mean, and dashed lines are the 5th and 95th prediction limits).

BOM website, were disaggregated. For Sydney, the first part of the data were used to estimate the model parameters, and the second part were used in the model validation. The model was validated using the maximum daily temperature (T) values associated to the dates of the R values. After the validation, the effect of temperature changes on the fine timescale statistics was examined. Finally, individual rainfall events of different R values were disaggregated using T values spanning the spectrum of the recorded data for the capital cities.

6.1. Aggregation of 24 h Wet Day Time Series

[61] The model was initially validated by comparing results of 100 simulations with the observed values at nine aggregation levels (0.1, 0.2, 0.5, 1, 2, 4, 8, 12, and 24 h) and on a monthly basis. This means the model parameters used in disaggregating daily rainfall amounts within the same month could be different depending on the maximum daily temperature value. At each aggregation level, the 100 simulations were averaged and the 5th and 95th percentiles were used to define the 90% prediction limits. Similarly, the IDF curves were established for several durations, defining the empirical probability as $P(X < x) = m/(N+1)$ where N is the number of years of records and m is the rank (lowest value ranked 1 and highest N) and the return period $\mathrm{Tr} = 1/(1-P)$. Figures 9 and 10 show some results for Darwin and Sydney (SDY2 data) which indicate that the observed statistics are very well preserved by the presented disaggregation model, noting that SYD2 data set was not used in the model parameter estimation. However, some

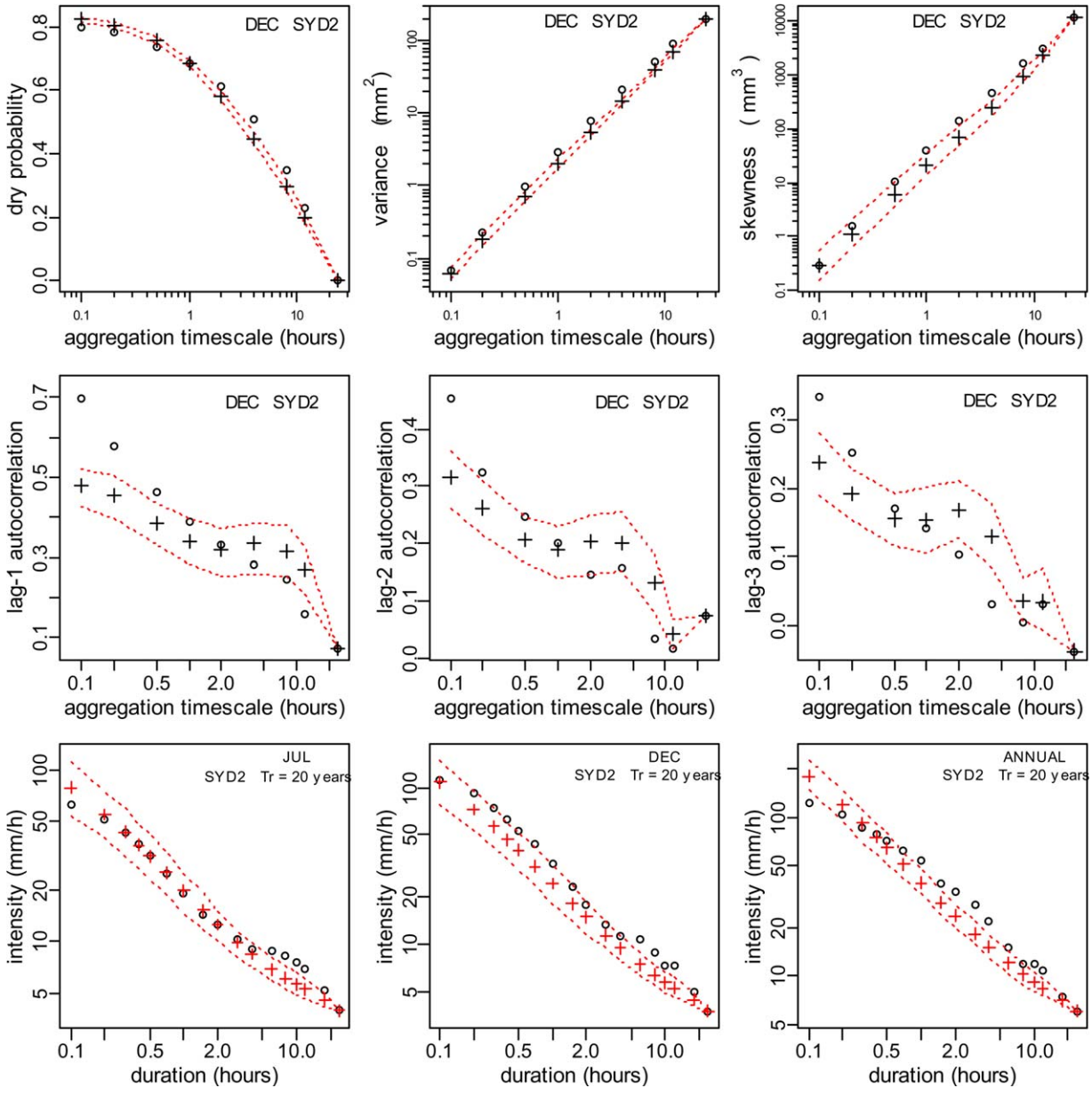

Figure 10. Comparison of the observed and simulated aggregation statistics and the intensity-duration-frequency (IDF) curves for SYD2 data set using parameters calibrated from SYD1 data set (circles are the observed values, pluses are the simulated mean, and dashed lines are the 5th and 95th prediction limits).

autocorrelations for timescales less than 0.5 h were underestimated for some months. Reproduction of the rainfall statistics were also evaluated for the extremes and middle temperature classes (1, 8, 16) of SYD2 data set. Their mean class temperatures are 15.0°C, 21.8°C, and 31.5°C, respectively. Figure 11 demonstrates that the presented daily rainfall disaggregation model works well under all temperature conditions.

[62] Being satisfied with the performance of the proposed model, it was used to evaluate changes in fine timescale rainfall statistics due to temperature changes. To achieve this aim, two sets of fine timescale rainfall time series were simulated from the observed daily totals. For the first set A, the observed temperature of the individual daily rainfall amounts was reduced by 1°C, and for the second set B, it was increased by 1°C. It needs to be underlined that the parameters depend on the temperature, and changes in temperature result in changes in the model's parameter set. Thus, the scenario investigated is where the same amount of rainfall occurred but at a 1°C increase or decrease in temperature. Then, the percentage rate of change, $P_{\%}$, of the statistics per 1°C rise in temperature was calculated as $P_{\%} = 100(B_{\text{stat}} - A_{\text{stat}})/(A_{\text{stat}} \times 2)$, where A_{stat} and B_{stat} are the averages of the statistic calculated for sets A and B, respectively, the temperature difference between the two data sets being 2°C. Table 11 provides the $P_{\%}$ values for 0.1, 0.5, and 1 h aggregation timescales which are considered to be crucial. Only the minimum,

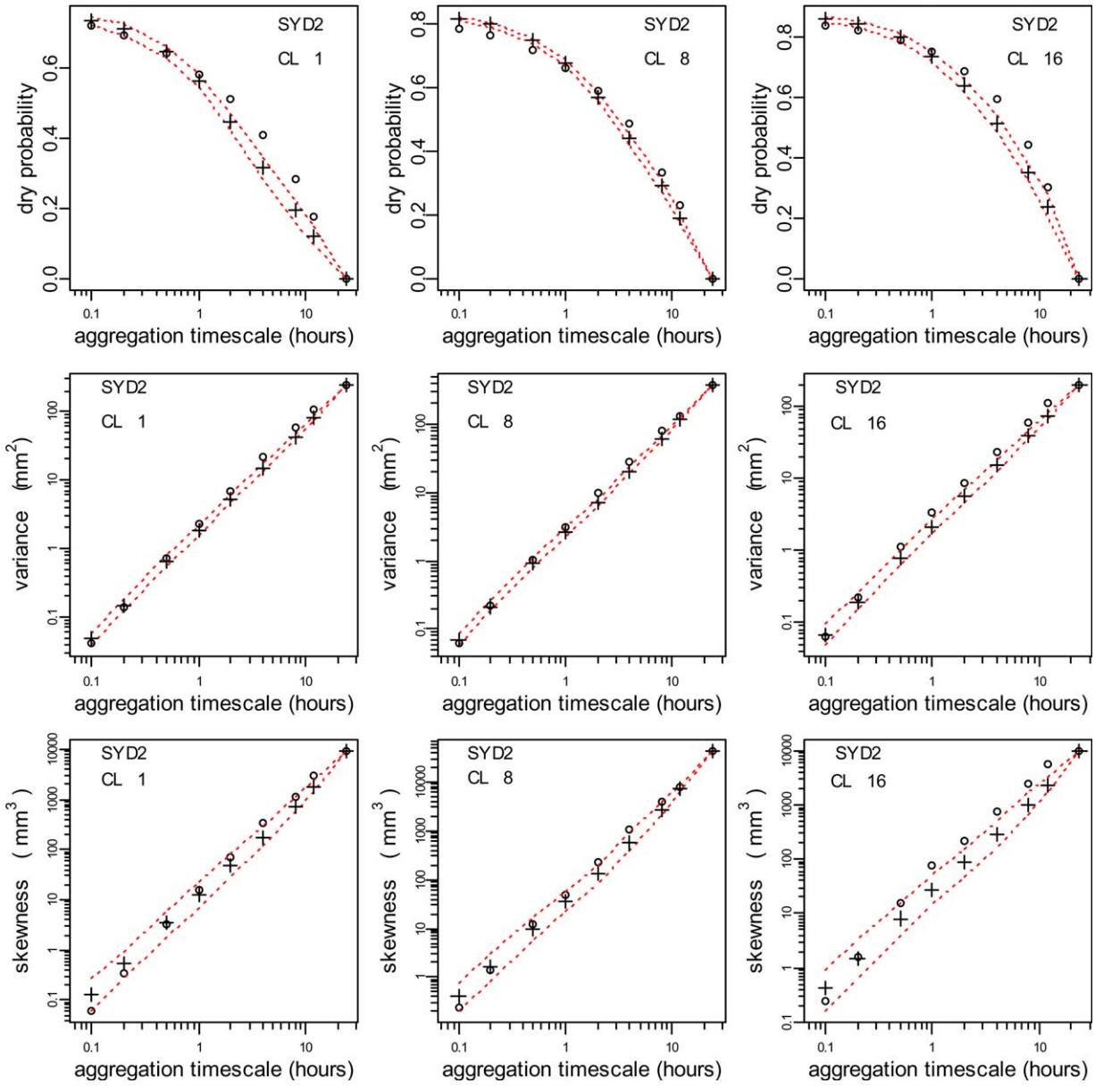

Figure 11. Comparison of some observed and simulated aggregation statistics of temperature classes 1 (mean = 14.96°C), 8 (mean = 21.76°C) and 16 (mean = 31.52°C) for SYD2 (circles are the observed values, pluses are the simulated mean, and dashed lines are the 5th and 95th prediction limits).

mean, and maximum of the monthly values for each statistic are shown due to space limitation. The same was done using the long-term daily rainfall records. The rates of change presented in Table 12 are very close to those in Table 11, and the small differences can be attributed to statistical variability.

[63] It is observed that the total wet periods' duration (and duration of events) and the autocorrelations decrease with increase in temperature, while the maximum proportional depth, variance, skewness, and the IDFs show an opposite effect. Also, the absolute values of $P_{\%}$ decrease with increasing aggregation level, with the exception of the autocorrelations. *Beuchat et al*. [2011] also observed similar trends of hourly rainfall time series dry proportion, variance, and skewness with temperature. Darwin, located in the tropics, exhibits the highest rates of change with total wet periods' duration, recording a mean of 14%, variance 16%, IDFs 9%, skewness 30%, and the autocorrelations 25%. Sydney, situated in a temperate region, recorded the lowest changes, registering a mean of 2% for total wet periods' duration, 5% for variance, 4% for autocorrelations, 10% for skewness, and 5% for the IDFs. Brisbane, located in the subtropics, gave values between those of Sydney and Darwin, registering a mean of 4% for total wet periods' duration, 7% for variance, 5% for autocorrelations, 18% for skewness, and 6% for the IDFs.

6.2. Single Event

[64] Storm profiles (i.e., ignoring leading and ending zeros within the 24 h day) were also analyzed and averaged over the total number of wet days within the months. For Sydney events, the variance rates of change range increased

Table 11. Percentage Rate of Change ($P_{\%}$) per 1°C Rise in Temperature of the Rainfall Statistics: Disaggregation of Daily Rainfall Derived From the 6 min Data Sets

	0.1 h Timescale			0.5 h Timescale			1 h Timescale		
Statistics	Min	Mean	Max	Min	Mean	Max	Min	Mean	Max
SYD2									
Wet duration	−3.0	−2.0	−1.4	−2.7	−1.9	−1.3	−2.4	−1.7	−1.2
Variance	0.9	3.5	7.7	0.6	2.7	6.0	0.3	2.4	5.4
Lag-1	−1.8	−1.0	−0.5	−2.3	−1.4	−0.4	−2.6	−1.6	−0.2
Lag-2	−2.3	−1.4	−0.4	−3.6	−2.0	−0.2	−4.0	−2.2	−0.4
Lag-3	−3.0	−1.7	−0.4	−4.1	−2.4	−0.4	−4.2	−2.0	−0.4
Skewness	1.0	7.8	20.3	1.2	7.1	13.3	3.0	6.6	12.8
Max 10 year	2.0	3.9	7.5	0.4	2.1	6.2	0.0	1.8	5.1
Max 20 year	1.5	4.0	9.8	0.5	2.4	6.6	0.0	1.7	5.2
DAR									
Wet duration	−15.0	−13.5	−11.7	−13.0	−12.0	−10.3	−11.4	−10.7	−9.0
Variance	12.3	16.2	17.7	11.0	13.8	15.3	10.3	12.6	14.5
Lag-1	−5.1	−2.3	−0.1	−4.5	−2.6	−1.0	−7.8	−5.1	−1.7
Lag-2	−4.4	−2.7	−1.5	−12.1	−7.6	−5.1	−23.3	−15.0	−9.4
Lag-3	−6.1	−3.5	−2.2	−17.3	−11.8	−7.7	−41.1	−21.8	−12.8
Skewness	15.8	30.2	36.1	17.8	25.9	31.2	16.7	24.1	29.3
Max 10 year	6.6	9.8	12.7	6.6	8.5	11.3	5.7	7.8	9.7
Max 20 year	6.4	8.3	10.6	5.3	7.8	10.0	5.4	7.8	10.4
BNE									
Wet duration	−4.4	−3.8	−2.5	−3.9	−3.4	−2.1	−3.6	−3.0	−1.9
Variance	5.1	6.8	8.6	4.2	5.8	6.8	4.2	5.2	5.9
Lag-1	−2.6	−1.1	−0.1	−2.7	−1.4	0.0	−3.0	−1.7	−0.7
Lag-2	−4.0	−1.7	−0.3	−4.6	−2.5	−0.8	−5.1	−3.2	−2.1
Lag-3	−4.3	−1.9	−0.5	−5.1	−3.2	−1.8	−6.5	−4.5	−3.1
Skewness	7.7	13.7	22.3	6.4	11.8	19.7	7.1	10.3	14.5
Max 10 year	2.5	5.1	9.1	2.7	4.4	6.2	2.9	4.3	5.6
Max 20 year	2.0	5.1	8.2	1.2	4.6	6.7	1.2	4.2	5.6

Table 12. Percentage Rate of Change ($P_{\%}$) per 1°C Rise in Temperature of the Rainfall Statistics: Disaggregation of Long Records of Daily Rainfall Data Sets

	0.1 h Timescale			0.5 h Timescale			1 h Timescale		
Statistics	Min	Mean	Max	Min	Mean	Max	Min	Mean	Max
SYD									
Wet duration	−3.0	−2.4	−2.0	−2.6	−2.1	−1.7	−2.3	−1.9	−1.6
Variance	2.8	5.0	8.3	2.5	4.0	6.4	2.2	3.5	5.7
Lag-1	−2.1	−1.2	−0.4	−2.0	−1.4	−0.9	−2.7	−1.7	−0.8
Lag-2	−2.9	−1.8	−0.6	−3.6	−2.3	−1.1	−4.9	−2.8	−1.6
Lag-3	−3.3	−2.1	−1.1	−4.8	−2.8	−1.2	−5.6	−3.4	−1.9
Skewness	5.3	10.2	20.3	4.2	7.4	13.4	3.7	6.7	12.4
Max 10 year	1.9	4.5	7.1	1.8	3.5	6.3	0.4	2.9	5.3
Max 20 year	1.8	4.7	6.8	1.8	3.6	6.2	1.2	3.1	5.4
DAR									
Wet duration	−14.2	−12.7	−10.9	−12.5	−11.2	−9.3	−10.9	−9.9	−7.7
Variance	11.7	15.3	16.3	9.1	13.0	15.0	7.6	11.9	13.8
Lag-1	−2.9	−2.1	−1.3	−4.1	−2.6	−0.8	−6.8	−5.0	−3.2
Lag-2	−4.3	−2.9	−1.3	−9.5	−7.2	−4.7	−25.8	−14.4	−9.8
Lag-3	−4.7	−3.5	−1.5	−16.3	−11.7	−7.5	−80.0	−24.7	−12.3
Skewness	15.3	28.0	33.5	12.8	23.7	30.5	9.2	22.0	27.7
Max 10 year	6.1	8.8	10.4	6.5	8.4	10.9	5.9	7.6	9.5
Max 20 year	5.3	8.6	13.2	6.2	7.7	9.3	5.9	7.4	9.6
BNE									
Wet duration	−4.8	−3.8	−2.5	−4.1	−3.4	−2.2	−3.7	−3.1	−2.0
Variance	5.0	7.7	9.6	4.0	6.2	8.4	3.6	5.7	7.7
Lag-1	−2.8	−1.5	−0.7	−2.9	−1.4	−0.4	−3.1	−1.8	−0.7
Lag-2	−3.8	−2.0	−0.7	−4.2	−2.4	−1.2	−5.4	−3.8	−2.6
Lag-3	−4.0	−2.3	−1.0	−4.6	−3.5	−1.8	−8.3	−5.3	−3.1
Skewness	11.2	18.0	27.8	9.2	13.6	22.2	6.6	12.7	19.5
Max 10 year	3.3	6.1	8.2	2.3	4.6	7.0	2.2	4.2	6.1
Max 20 year	2.3	5.9	9.6	2.0	4.8	7.8	1.3	4.6	7.1

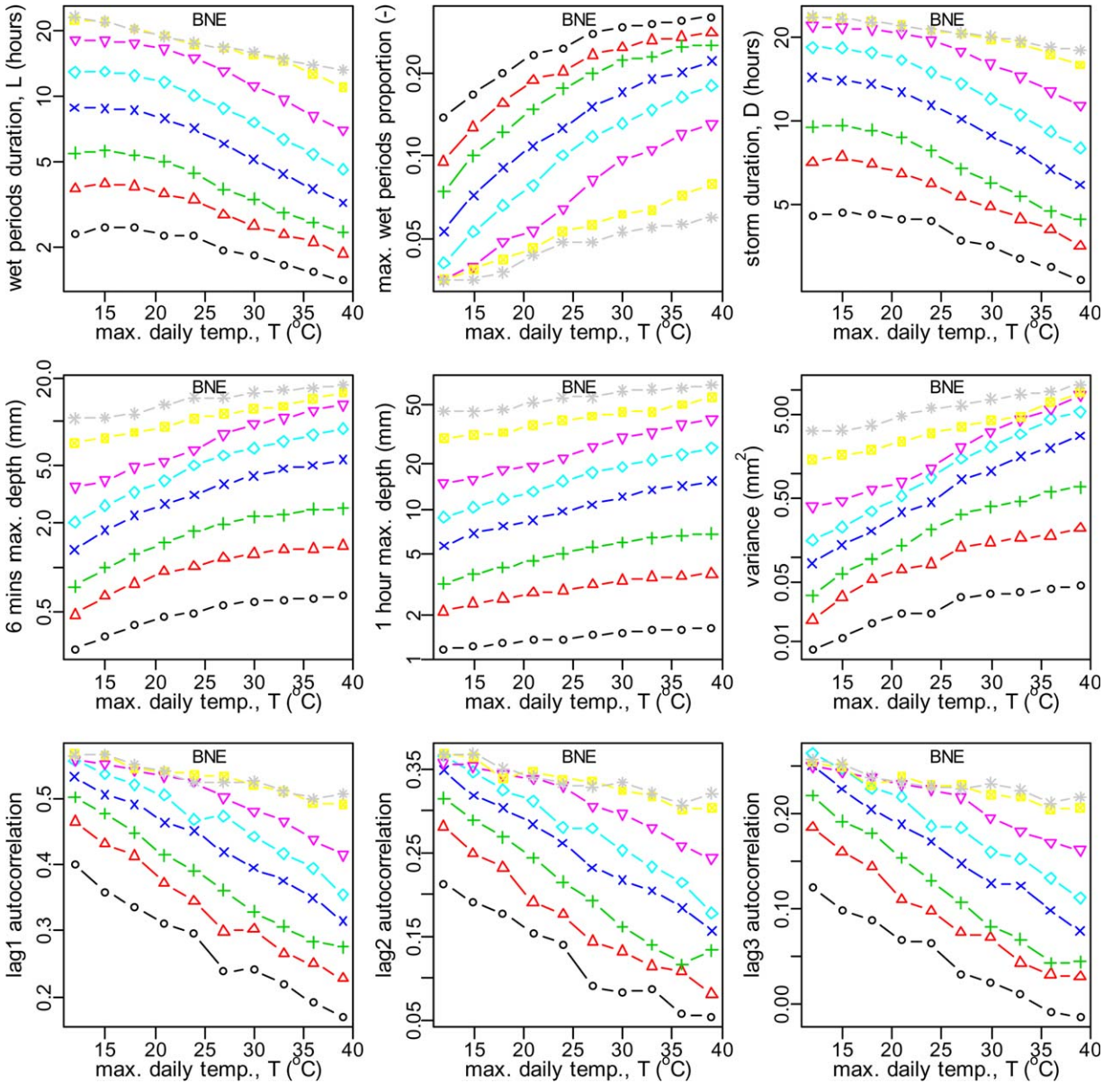

Figure 12. Single event: variation of the average values of the statistics with temperature (T) for different daily rainfall amounts (R) contained in {2,5,10,25,50,100,200,300 mm}, for Brisbane, 2 mm (circles, black) and 300 mm (asterisks, brown).

to 10% and the skewness to 14%. The estimated increases for Brisbane were to 14% for variance and to 26% for skewness. Darwin, situated in the tropics, registered the highest variability of 40% for variance and 53% for skewness.

[65] To properly investigate the temperature effects on single events, R values within the set {2, 5, 10, 25, 50, 100, 200, 300 mm} were each disaggregated 1000 times and at 10 different but equally spaced temperatures within the recorded range of the capital cities. The relevant statistics were estimated for each storm profile simulated. Figure 12 shows the variation of the average of the 1000 simulations for each T-R pair values for Brisbane. The general trend of the rate of change of the statistics is similar to what was observed using the observed daily rainfall time series. Note that the increase in M with temperature and the decrease in D with temperature lead to an increase in the maximum period depths. For the event scenario, the rates of change per 1°C rise in temperature along each R-T curve were calculated, and the averages of these values are presented in Table 13.

[66] With the exception of the autocorrelations, the statistics exhibit a marginal increase in the numerical value of the rates of change up to R values between 25 and 50 mm before again marginally decreasing with further increase in R. The autocorrelations show a clear decreasing trend with R. Sample size and statistical variability could be sources of the observed nonmonotonic change in the statistics presented in Table 13. Basing the argument on the average values of the statistics over R, the rate of change of L with temperature varies from 2% to 12% from a temperate climate to the tropics, 4% to 8% for M, 1% to 10% for D, 4%

Table 13. Percentage Rate of Change per 1°C Rise in Temperature of the Rainfall Statistics for Single Events, and Considering Temperature Values Within the Recorded Range of the Capital Cities[a]

R (mm)	L	M	D	0.1 h Max	1 h Max	V	S	Lag-1	Lag-2	Lag-3
SYD										
2	−1.0	3.5	−1.3	3.5	1.3	12.0	22.4	−2.7	−2.5	−4.1
5	−2.0	4.2	−1.8	4.1	2.0	15.1	29.8	−1.6	−2.1	−3.2
10	−2.3	4.1	−1.8	4.0	2.9	13.1	26.1	−1.1	−1.5	−1.8
25	−2.3	4.7	−1.2	4.7	2.9	10.4	29.0	−0.9	−1.2	−1.5
50	−2.0	4.4	−0.8	4.4	2.7	10.1	22.5	−0.6	−0.6	−0.6
100	−2.0	4.1	−0.5	4.1	2.6	6.9	16.2	−0.4	−0.2	−0.7
200	−2.0	3.2	−0.4	3.2	2.2	5.5	8.8	−0.3	−0.2	−0.8
300	−1.8	2.5	−0.4	2.5	2.1	4.6	7.2	−0.2	−0.7	−0.5
Mean	−1.9	3.8	−1.0	3.8	2.3	9.7	20.3	−1.0	−1.1	−1.7
DAR										
2	−10.7	6.9	−9.3	6.9	2.8	17.1	17.5	−21.1	−27.2	−47.7
5	−12.2	6.5	−11.6	6.5	3.9	19.3	21.0	−19.6	−29.6	−37.1
10	−11.3	7.2	−10.0	7.2	4.9	25.2	29.7	−14.2	−21.1	−19.9
25	−11.3	8.3	−9.6	8.2	6.1	28.8	34.6	−8.0	−12.8	−19.0
50	−12.8	10.6	−10.8	10.6	8.0	39.5	50.2	−7.8	−12.1	−10.9
100	−13.4	10.3	−11.2	10.2	9.5	35.5	44.7	−5.9	−9.5	−15.1
200	−12.6	8.1	−9.9	8.1	9.2	27.2	32.9	−4.1	−6.0	−7.5
300	−11.5	6.4	−9.1	6.5	8.0	22.1	26.6	−2.9	−4.1	−5.3
Mean	−12.0	8.0	−10.2	8.0	6.6	26.8	32.2	−10.5	−15.3	−20.3
BNE										
2	−2.6	3.3	−2.5	3.3	1.2	7.3	11.4	−3.5	−4.3	−9.4
5	−3.3	4.4	−3.1	4.4	2.2	11.5	19.0	−2.7	−4.2	−6.1
10	−3.7	5.0	−3.3	5.0	3.0	13.6	23.2	−2.2	−3.9	−6.0
25	−3.5	5.8	−3.1	5.8	3.9	16.3	23.6	−1.9	−2.8	−4.1
50	−4.4	6.1	−2.9	6.0	4.2	16.2	25.8	−1.8	−2.5	−3.0
100	−3.3	5.2	−2.3	5.2	3.8	13.8	21.3	−1.1	−1.4	−1.6
200	−2.6	3.1	−1.4	3.1	2.4	7.7	10.4	−0.5	−1.1	−1.4
300	−2.0	2.0	−1.0	2.2	1.9	5.1	8.4	−0.8	−0.9	−1.0
Mean	−3.2	4.4	−2.5	4.4	2.8	11.4	17.9	−1.8	−2.6	−4.1

[a]*R*, daily rainfall amount; *L*, total wet periods' duration; *M*, maximum wet period proportional depth; *D*, duration of the storm event; *V*, variance; *S*, skewness.

to 8% for maximum wet periods' depth, 10% to 26% for variance, 20% to 32% for skewness, and 1% to 20% for the autocorrelations. For the observed daily rainfall time series case, the statistics were calculated for the 24 h day including the leading and ending zeros and averaged over several values, thus decreasing the values of the rates of change of the statistics such as the variance and skewness. However, the events' rates of change are consistent with the observed daily rainfall time series cases.

[67] The observed patterns of the effects of temperature on the fine timescale rainfall statistics is supported by the general perception that global warming will lead to intensification of rainfall events as a result of an increase in variance, a decrease in total wet periods' duration (and event duration), and autocorrelation [e.g., *Meehl et al*., 2007; *Lenderink and van Meijgaard*, 2008]. This is believed to be the case even for regions where mean rainfall is decreasing with temperature (e.g., most subtropical and midlatitude regions). Using a high-resolution regional climate model, *Lenderink and van Meijgaard* [2008] showed that 1 h precipitation extremes increase at a rate close to 14% per degree of warming in large parts of Europe.

7. Summary

[68] An enhanced copula-based daily rainfall disaggregation model is presented. Specifically, the novelties and improvements over the model presented by *Gyasi-Agyei* [2011] are

[69] (1) the rainfall data are grouped using daily temperature quantiles instead of the usual monthly grouping to account for seasonal temperature shifts;

[70] (2) the model parameters are explicitly conditioned on maximum daily temperature to allow evaluation of temperature changes on fine timescale rainfall statistics, and this is supported by the empirical evidence presented;

[71] (3) the wet/dry binary indicator submodel is calibrated only on the storm profile, ignoring the leading and ending zeros of the 24 h day, thereby improving the performance of the model and also shortening the simulation time;

[72] (4) incorporation of storm profile types allows accurate modeling of consecutive wet days;

[73] (5) the range of copulas, including metaelliptic, and marginal distributions types have been expanded; and

[74] (6) the total wet periods' duration, the maximum wet period proportional depth random variables, and the ρ statistics of the wet periods' depth are transformed to the positive real line to significantly improve the marginal distributions fitting by the maximum likelihood method.

[75] Empirical investigation of temperature scaling with the three major storm profile random variables, whose joint probability distribution is captured by copulas, was examined for several percentiles to support the conditioning of the model parameters on temperature. It is observed that

the exponential rate of change of the random variables is very significant, particularly for the hot climates with values over 15%.

[76] The applicability of the proposed disaggregation model to evaluate the rates of change of fine timescale rainfall statistics with temperature has been demonstrated using two daily rainfall data sets for three Australian capital cities located in different climatic regions. Simulation results have indicated that statistics such as the total wet periods' duration, storm event duration, and the autocorrelations decrease with increase in temperature, while the maximum proportional depth, variance, skewness, and the IDFs show an increasing trend with temperature. Quantitatively, it is shown that on average, a 1°C rise in temperature could cause mean rates of change in the statistics depending on the climate, and for the aggregated 24 h rainfall time series case was

[77] (1) the tropical region: total wet periods' duration 14%, variance 16%, IDFs 9%, skewness 30%, autocorrelations 25%;

[78] (2) the subtropical region: total wet periods' duration 4%, variance 7%, IDFs 6%, skewness 18%, autocorrelations 5%; and

[79] (3) the temperate region: total wet periods' duration 2%, variance 5%, IDFs 5%, skewness 10%, autocorrelations 4%.

[80] For single events of varying R values, and considering only the storm profile, the rates of change from temperate to tropical climates were estimated as ranging from 2% to 12% for total wet periods' duration (and for event duration), 4% to 8% for maximum wet period depth, 10% to 26% for variance, 20% to 32% for skewness, and 1% to 20% for the autocorrelations.

[81] The improved disaggregation model is independent of the month, and all that is required is the maximum daily temperature which is available with the daily rainfall data to be disaggregated. There is a high potential to use the presented model for forecasting as the maximum daily temperature can be predicted with a very high accuracy. Future work will explore incorporation of other atmospheric variables and climate indices.

[82] **Acknowledgments.** Constructive comments by Geoff Pegram and two anonymous reviewers are gratefully acknowledged.

References

Aas, K., C. Czado, A. Frigessi, and H. Bakken (2009), Pair-copula constructions of multiple dependence, *Insurance: Math. Econ.*, *44*, 182–198.

Bedford, T., and R. M. Cooke (2001), Probability density decomposition for conditionally dependent random variables modeled by vines, *Ann. Math. Artif. Intel.*, *32*, 245–268.

Bedford, T., and R. M. Cooke (2002), Vines—A new graphical model for dependent random variables, *Ann. Stat.*, *30*, 1031–1068.

Berg, P., J. O. Haerter, P. Thejll, C. Piani, S. Hagemann, and J. H. Christensen (2009) Seasonal characteristics of the relationship between daily precipitation intensity and surface temperature, *J. Geophys. Res.*, *114*, D18102, doi:10.1029/2009JD012008.

Beuchat, X., B. Schaefli, M. Soutter, and A. Mermoud (2011), Toward a robust method for subdaily rainfall downscaling from daily data, *Water Resour. Res.*, *47*, W09524, doi:10.1029/2010WR010342.

Bo, Z., S. Islam, and E. A. B. Eltahir (1994), Aggregation-disaggregation properties of a stochastic rainfall model, *Water Resour. Res.*, *30*(12), 3423–3435, doi:10.1029/94WR02026.

Cowpertwait, P. S. P., P. E. O'Connell, A. V. Metcalfe, and J. A. Mawdsley (1996), Stochastic point process modelling of rainfall. Single-site fitting and validation, *J. Hydrol.*, *175*, 17–46.

De Michele, and C., G. Salvadori (2003), A generalized Pareto intensity-duration model of storm rainfall exploiting 2-Copulas, *J. Geophys. Res.*, *108*(D2), 4067, doi:10.1029/2002JD002534.

Econopouly, T. W., D. R. Davis, and D. A. Woolhiser (1990), Parameter transferability for a daily rainfall disaggregation model, *J. Hydrol.*, *118*, 209–228.

Fang, H. B., Fang, K. T., and S. Kotz. (2002), The meta-elliptical distributions with given marginals, *J. Multivariate Anal.*, *82*, 1–16.

Gallant, A. J. E., A. S. Kiem, D. C. Verdon-Kidd, R. C. Stone, and D. J. Karoly (2012), Understanding hydroclimate processes in the Murray-Darling Basin for natural resources management, *Hydrol. Earth Syst. Sci.*, *16*, 2049–2068.

Genest, C., A. C. Favre, J. Béliveau, and C. Jacques (2007), Metaelliptical copulas and their use in frequency analysis of multivariate hydrological data, *Water Resour. Res.*, *43*, W09401, doi:10.1029/2006WR005275.

Glasbey, C. A., G. Cooper, and M. B. McGechan (1995), Disaggregation of daily rainfall by conditional simulation from a point-process model, *J. Hydrol.*, *165*, 1–9.

Gyasi-Agyei, Y. (1999), Identification of regional parameters of a stochastic model for rainfall disaggregation, *J. Hydrol.*, *223*(3–4), 148–163.

Gyasi-Agyei, Y. (2005), Stochastic disaggregation of daily rainfall into one-hour time scale, *J. Hydrol.*, *309*, 178–190.

Gyasi-Agyei, Y. (2011), Copula-based daily rainfall disaggregation model, *Water Resour. Res.*, *47*, W07535, doi:10.1029/2011WR010519.

Gyasi-Agyei, Y. (2012), Use of observed scaled daily storm profiles in a copula based rainfall disaggregation model, *Adv. Water Resour.*, *45*, 26–36.

Gyasi-Agyei, Y., and P. B. Mahbub (2007), A stochastic model for daily rainfall disaggregation into fine time scale for a large region, *J. Hydrol.*, *347*, 358–370.

Gyasi-Agyei, Y., and C. S. Melching (2012), Modelling the dependence and internal structure of storm events for continuous rainfall simulation, *J. Hydrol.*, *464–465*, 249–261.

Gyasi-Agyei, Y., and G. R. Willgoose (1997), A hybrid model for point rainfall modelling, *Water Resour. Res.*, *33*(7), 1699–1706, doi:10.1029/97WR01004.

Gyasi-Agyei, Y., and G. R. Willgoose (1999), Generalisation of a hybrid model for point rainfall, *J. Hydrol.*, *219*(3–4), 218–224.

Hardwick-Jones, R., S. Westra, and A. Sharma (2010), Observed relationships between extreme sub-daily precipitation, *surface temperature and relative humidity*, Geophys. Res. Lett., 37, L22805, doi:10.1029/2010GL045081.

Hershenhorn, J., and D. A. Woolhiser (1987), Disaggregation of daily rainfall, *J. Hydrol.*, *95*, 299–322.

Ho, M., A. S. Kiem, and D. C. Verdon-Kidd (2012), The southern annular mode: A comparison of indices, *Hydrol. Earth Syst. Sci.*, *16*, 967–982.

Joe, H. (1996), Families of m-variate distributions with given margins and $m(m-1)/2$ bivariate dependence parameters, in *Distributions With Fixed Marginals and Related Topics, Monogr. Ser.*, vol. *28*, edited by L. Ruschendorf, B. Schweizer, and M. D. Taylor, pp. 121–141, Inst. of Math. Stat. Lect. Notes, Hayward, Calif.

Joe, H. (1997), *Multivariate Models and Dependence Concepts*, Chapman and Hall, London, U. K.

Kao, S. C., and R. S., Govindaraju (2008), Trivariate statistical analysis of extreme rainfall events via the Plackett family of copulas, *Water Resour. Res.*, *44*, W02415, doi:10.1029/2007WR006261.

Koutsoyiannis, D., and C. Onof (2001), Rainfall disaggregation using adjusting procedures on a Poisson cluster model, *J. Hydrol.*, *246*, 109–122.

Krajewski, W. F., G. Villarni, and J. A. Smith (2010), Radar-rainfall uncertainties, *Bull. Am. Meteorol. Soc.*, *91*, 87–94.

Lenderink, G., and E. van Meijgaard (2008), Increase in hourly precipitation extremes beyond expectations from temperature changes, *Nat. Geosci.*, *1*, 511–514.

Meehl, G. A. et al. (2007), Global climate projections, in *Climate Change 2007: The Physical Science Basis. Contribution of Working Group I to the Fourth Assessment Report of the Intergovernmental Panel on Climate Change*, Cambridge Univ. Press, Cambridge, U. K.

Molnar, P., and P. Burlando (2005), Preservation of rainfall properties in stochastic disaggregation by a simple random cascade model, *Atmos. Res.*, *77*, 137–151.

Nelson, R. B. (2006), *An Introduction to Copulas*, 2nd ed., Springer, New York.

Palynchuk, A., and Y. Guo (2011), A probabilistic description of rain storm incorporating peak intensities, *J. Hydrol.*, *409*, 71–80.

Press, W. H., S. A. Teukolsky, W. T. Vetterling, and B. P. Flannery (2007), *Numerical Recipes: The Art of Scientific Computing*, 3rd ed., 1286 pp., Cambridge Univ. Press, N. Y.

Rodriguez-Iturbe, I., D. R. Cox, and V. Isham (1987), Some models for rainfall based on stochastic point processes, Proc. R. Soc. London A, *410*, 269–288.

Salvadori, G., C. De Michele, N. Kottegoda, and R. Rosso (2007), *Extremes in Nature: An Approach Using Copulas, Water Sci. Technol. Libr. Ser.*, vol. *56*, Springer, Dordrecht, Netherlands.

Serinaldi, F., and S. Grimaldi (2007), Fully nested 3-copula: Procedure and application on hydrological data, *J. Hydrol. Eng.*, *12*(4), 420–430.

Trenberth, K. E. (2011), Changes in precipitation with climate change, *Clim. Res.*, *47*, 123–138.

Vandenberghe, S., N. E. C., Verhoest, and B. De Baets (2010), Fitting bivariate copulas to the dependence structure between storm characteristics: A detailed analysis based on 105-year 10 min rainfall, *Water Resour. Res.*, *46*, W01512, doi:10.1029/2009WR007857.

Westra, S., R. Mehrotra, A. Sharma, and R. Srikanthan (2012), Continuous rainfall simulation: 1. A regionalized subdaily disaggregation approach, *Water Resour. Res.*, *48*, W01535, doi:10.1029/2011WR010489.

Wooten, R. D. (2011), Statistical analysis of the relationship between wind speed, pressure and temperature, *J. Appl. Sci.*, *11*(15), 2712–2722.

Zhang, L., and V. P. Singh (2007) Gumbel-Hougaard copula for trivariate rainfall frequency analysis, *J. Hydrol. Eng.*, *12*(4), 409–419.